Towards green transition of touristic islands through hybrid renewable energy systems. A case study in Tenerife, Canary Islands

Towards green transition of touristic islands through hybrid renewable energy systems. A case study in Tenerife, Canary Islands.

Elisa Dallavalle[1], Mariasole Cipolletta[1], Valeria Casson Moreno[1], Valerio Cozzani[1], Barbara Zanuttigh[1]

(1) University of Bologna, Department of Civil, Chemical, Environmental and Materials Engineering, Viale del Risorgimento 2, 40136 Bologna, Italy
elisa.dallavalle3@unibo.it, mariasole.cipolletta@unibo.it, valeria.cassonmoreno@unibo.it, valerio.cozzani@unibo.it, barbara.zanuttigh@unibo.it

Abstract

The Canary Islands are still largely dependent on expensive imported fossil fuels, are stressed by the increasing touristic impact and are extremely vulnerable to climate change due to water scarcity. Water desalinisation is an energy-demanding process and is essential to the sustainable development of these islands. The aim of this study is to explore the potential advantages of a hybrid installation, exploiting two different renewable energy sources, specifically waves and solar, to supply a large desalination plant in Tenerife. The paper ultimately provides a generally applicable procedure for the design of hybrid installations, including three steps: the assessment of available renewable energy sources, the optimal combination of these sources and finally the economic assessment. The wave and solar resources are assessed first, then the hybrid installation is conceptually designed proposing a criterion for the optimal mixing of the renewable energy sources that can be applied to other resources and other sites. The basic idea is to maximize the exploitation of the renewable power, minimizing the need of the fossil-based back-up system. The costs of the hybrid installation are finally assessed considering the sensitivity to government incentives, showing that the project parity point is reached within the lifetime of typical desalination plants (i.e. 40 years) and can be significantly more attractive in case of Feed-In-Tariffs available in other European countries.

Keywords

Hybrid installation; energy mixing; wave energy; solar energy; desalination; cost assessment.

1. Introduction

A significant contribution to climate change adaptation may come from marine renewable energy production and from innovative multi-functional offshore installations that may shift offshore part of the anthropogenic pressures (e.g. tourism, aquaculture) on coastal systems (Zanuttigh et al., 2015, 2016). Unlocking the potential of marine resources is crucial to achieve the green energy production goals while preserving the vulnerable marine ecosystem and responding to the increasing demand for energy, food and transportation. Some conversion technologies are consolidated and widely applied, such as fixed wind energy plants, that however cannot be placed in very deep waters, as they require to be drilled in the seabed, with some environmental impact together with some aesthetic impact depending on the distance from shore (Lüdeke, 2017; Durning and Broderick, 2019). Floating wind farms, that can overcome these problems, are under testing, due to the challenging stability issues in extreme conditions (Kausche et al., 2018; Moore et al., 2018; Hannon et al., 2019). Wave energy harvesting is far from being economically feasible, mainly due to the low-efficient technologies of power conversion (Drew et al., 2009) and to design challenges such as the moorings design (Harris et al., 2006; Martinelli and Zanuttigh, 2018). Floating PV-panels have been already installed on pond and lakes and have still to overcome the challenge of the harsh off-shore conditions (Trapani and Redón-Santafé, 2015; Sahu, et al., 2016).

In this context, previous research (FP7 MARINA, ORECCA and SOFIA projects) and prototype testing suggested the combination of different sources of marine Renewable Energy Sources (RES) to increase the active operational time and the economic feasibility of these plants. The potential of combined installations of wind and wave energy has been studied by many authors, among others Fernandez-Chozas et al. (2012), Astariz et al. (2015), Zanuttigh et al. (2015), Contestabile et al. (2017). A review can be found in (Perez Collazo et al., 2015).

Demonstrations of integrated plants have been poorly performed so far, experiences being limited to a few prototypes integrating wind and wave energy, while many conceptual designs at different level of detail do exist (Nassar et al., 2020). New frontiers are being explored with the Wind Power Hub project (2016): a “green” island, consisting of fixed wind piles with a capacity of several GWs, solar panels, plus an airport and a harbour for operation, is expected to be built up on the Dogger Bank by 2050.

Three key original observations are at the basis of this contribution.

64 The first is that wave energy and wind energy are more frequently contemporary rather than
65 complementary, especially in limited-fetch seas, and therefore it is likely that the combination of
66 wind or wave with sun would allow to cover the energy needs at a given site for a longer period,
67 since these sources are naturally "in opposition of phase" as the first ones are maxima during storms
68 and the latter achieves its peak during good weather.

69 The second is that there are many populated islands (2'200 only in the European Union), most of
70 which depend on expensive fossil fuel imports for their energy supply. Many of these islands do also
71 experience problems with transportation and heat, especially during the stormy season, and are
72 exposed to water scarcity, especially during the touristic season, while being naturally placed in
73 high-energy locations. The *Clean energy for EU islands* initiative (2017; 2020), launched in 2017,
74 provides a long-term framework to support their sustainable development by increasing the
75 production of renewable energy. This in turns leads to the reduction of environmental impacts, the
76 creation of new jobs and business opportunities, the increase of energy security due to lower need
77 for imports, and overall, to the improvement of the islands' economic self-sufficiency.

78 The third is that the combination of renewables is indeed a challenge for energy grids, due to energy
79 variability, uncertainty, non-synchronous generation, low-capacity factor and distance of the
80 generation site from the grid.

81 This paper integrates for the first time these three observations by analysing the feasibility of
82 renewable energy transition for touristic islands, with application to Tenerife, in the Canary Islands.
83 Specifically, the combination of off-shore wave and on-shore solar energy to locally supply a water
84 desalination plant is analysed. An objective criterion for the optimal mixing of the RES is proposed
85 to allow for a general application to other RES and for exportability to other sites.

86 The paper starts from an overview of the site in Section 2, considering the environmental, social and
87 economic conditions. The selection of wave and solar energy, among the available RES, is also
88 motivated. Section 3 analyses the available wave energy, including seasonality, and the potential
89 power production based on one of the more mature technologies for energy conversion. A similar
90 assessment is performed for solar energy in Section 4. The optimal RES mixing to power the
91 desalination plant is described in Section 5. The economic assessment is carried out in Section 6, in
92 terms of the prices required to wave energy to make economically viable the implementation of the
93 hybrid power generation plant. Conclusions are drawn in Section 7.

2. Description of the study area

The aim of this Section is to provide a description of Tenerife Island, including environmental, social and economic characteristics (Sub-section 2.1). The energy demand and the RES availability is also specifically addressed (Sub-section 2.2), including the reasons for selecting wave and solar energy as the most suitable RES to be investigated in the present study.

2.1 Overview of the site

Tenerife is the largest, highest and most populated of the Canary Islands, with a land area of about 2'000 km^2, a maximum elevation that exceeds 3'700 m and more than 900'000 inhabitants at the start of 2019 (Real Decreto, 2018). Moreover, it is also the most visited island of the archipelago, with approximately 5M tourists per year and a distributed touristic pressure of about 480'000 visitors per month (Gobierno de Canarias, 2020b).

Tenerife hosts many natural heritage observation, conservation and protection areas (Cabildo de Tenerife, 2019), such as national and natural parks, different types of natural reserves, and sites of scientific interest as depicted in Figure 1. With regard to marine conservation areas, Hernandez et al. (2007) classified Tenerife as a Highly Fished Area (HFA), thus outside Marine Protected Areas (MPA). At present, there are some MPAs in the South-East of the Island and only one MPA near the coast in the North-East of Tenerife, Anaga (Figure 1), which covers only 8 km^2 (Marine Protection Atlas). The vast majority of the observations of cetaceans between the years 1997 and 2006 were recorded along the South-West coast of Tenerife, while few sightings were recorded along the North-East coast of the Island (Carrillo et al., 2010).

From a geological point of view, Tenerife lies on a volcanically active zone with narrow and steep continental shelf, due to the presence of the sleeping volcano of Mount Teide. Debris avalanche deposits are present offshore Tenerife and many avalanche events were mapped offshore the Northern coast (Llanes et al., 2003).

Climate in the Canary Islands is mild, due to the influence of the North-North East trade winds and the cool waters of the subtropical North Atlantic. However, cool trade wind episodically weakens and easterly Saharan air reaches the Canaries, causing heatwaves with daily temperatures up to 45° C, drops in relative humidity down to 15% and the presence of suspended desert dust (Dorta, 2007).

The Canary Islands are characterized by extreme aridity as precipitations are scarce and irregular (Rosales-Asensio et al., 2020). After the over-exploitation of the aquifers, water desalination has been constantly increasing over the last decades to face the development of agriculture, the increase of tourism and the population growth (Rosales-Asensio et al., 2020). Almost the 30% of fresh water in the Canary Islands comes from desalination plants, with a peak of the 99% in Lanzarote (Rosales-Asensio et al., 2020; Garcia-Rubio and Guardiola, 2012).

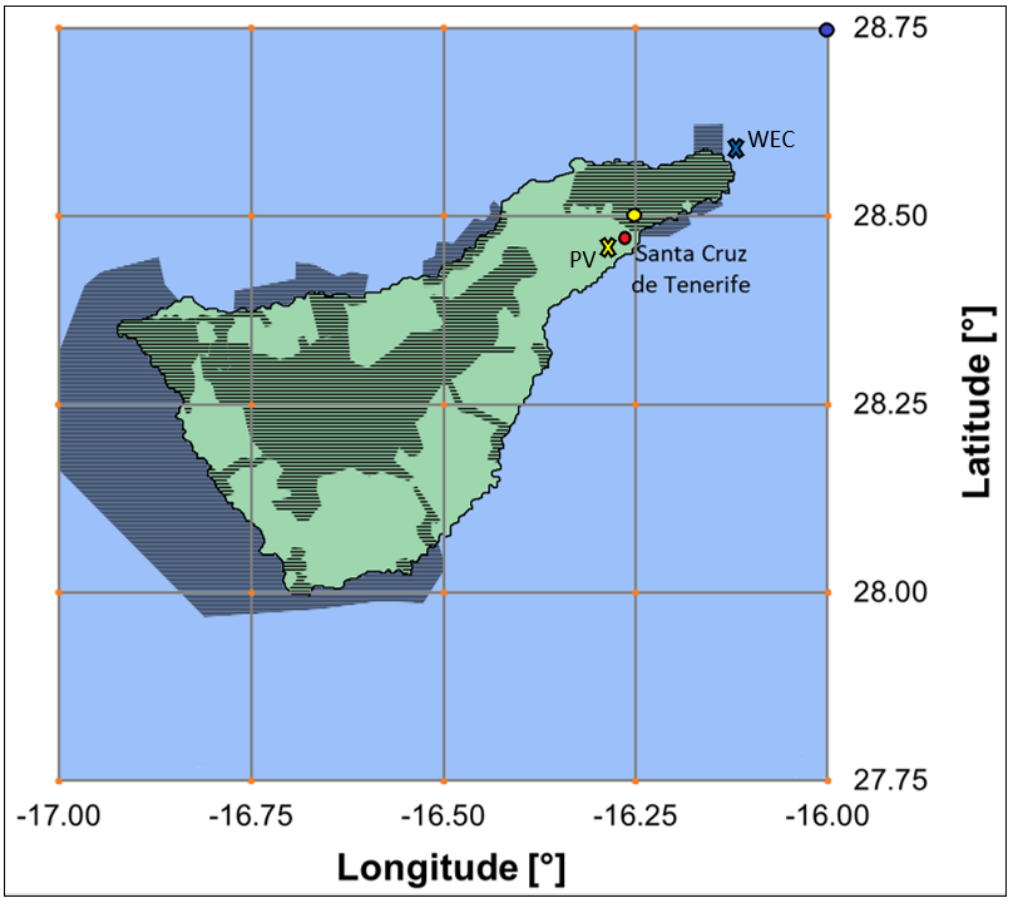

Figure 1. Map of Tenerife: the striped pattern indicates natural parks, reserves and MPA. The intersections of the geographical grid correspond to the points where solar data are available (Sub-section 4.1). The blue and the yellow filled-in circles indicate respectively the positions in which wave and solar data are collected, while the blue and the yellow crosses individuate the locations for the WEC and the PV plant respectively (Sub-sections 3.1 and 4.1).

Nowadays, 299 desalination plants, mostly using Reverse Osmosis (RO) technology, are operating in the Canary Islands, with a desalinated water volume of about 250 hm^3/year (Rosales-Asensio et al.,

2020). In Tenerife, there are 46 desalination plants with a total production of about 40 hm^3/year, covering the 9% of the total water demand of the island.

2.2 The energy scenario in Tenerife

At present, only the 8% of the electrical power in the Canary Islands comes from RES, specifically onshore wind and solar photo-voltaic, 153 MW and 166 MW respectively in 2016 (CEICC, 2016). Thus, the islands are significantly affected by fossil fuel price shocks and this threat is perceived by social actors as more relevant than climate change issues (Hernandez et al., 2018). Indeed the cost of energy in the Canary Islands ranges from a minimum of 0.18 €/kWh in Tenerife up to a maximum of 0.26 €/kWh in El Hierro, which is 3.5 times the prices at the Peninsula, an extra charge that does not impact local consumers, but is rather spread around all Spanish energy consumers (Schallenberg-Rodríguez and García Montesdeoca, 2018).

The energy consumption in Tenerife was estimated to be 4.173 kWh per capita in 2016, very close to the Spanish one of 5.692 kWh per capita (Gobierno de Canarias, 2017). The same year, the electric generation capacity on the Island exceeded 1200 MW, of which approximately the 93% was petroleum-derived (mainly through thermal power stations) and only 154 MW were obtained from RES. The main RES contribution is solar energy (74.6%), the second is on-shore wind energy (23.8%) and the rest is provided by mini-hydraulic installations and biogas plants (Gobierno de Canarias, 2017).

To increase the sustainable development in Tenerife, the potential of new RES installations is examined. There are no additional potential locations for onshore wind farms in the Canary Islands, as a consequence of the peculiarity of the territory combined with the legislative limits and with the aesthetic impact (Schallenberg-Rodríguez and Notario-del Pino, 2014). The legislation is less restrictive for on-shore solar plants than for wind farms (Schallenberg-Rodríguez and Notario-del Pino, 2014). Based on the present land use, over 48% of the total land belongs to natural reserves (Cabildo de Tenerife, 2019), but around the 21% of Tenerife's area would be eligible for solar plants (Schallenberg-Rodríguez and García Montesdeoca, 2018).

Schallenberg-Rodriguez and Montesdeoca (2018) explored areas for offshore bottom-fixed and floating wind installation, finding nearly the 12% of the territorial waters available for such purpose, and estimated a power production up to 180 TWh per year (i.e. around 22 times the total annual energy consumption of the Canary Islands). According to these authors, Fuerteventura, Lanzarote,

Gran Canaria, and Tenerife could be fully powered by the energy generated by traditional fixed turbines installed at a depth of 50 m, while La Palma and El Hierro would mainly depend on floating turbines.

After Schallenberg-Rodriguez and Montesdeoca (2018), the only option of off-shore fixed wind energy would be economically viable for Tenerife. However, despite promising, off-shore wind energy was not considered in this study because of the piles environmental impact, of the low social acceptability caused by the visual impact and because of the submarine daily seismic activity (Carniel et al., 2008; Volcano Discovery, 2020).

Following the outcomes of previous research on multi-use marine platforms in the Canary Islands (a.o. the FP7 TROPOS and the H2020 MUSES European projects), the marine renewable installation will be a floating installation and will consist of a single unit or an array of wave energy devices (Section 3). Wave energy will be combined with a new installation of solar on-shore plant (Section 4). The integration of these resources will then be considered to provide the power supply to the water desalinisation plant (Section 5).

Due to the proximity between the energy source and the infrastructure and considering the issues related to the connection to the grid, the option to supply a desalination plant with energy recovered by wave energy converters (WECs) was found to be an interesting solution (e.g. Franzitta et al., 2016; Leijon and Bostrom, 2018). Fernandez-Prieto et al. (2019), in particular, examined the opportunity to use wave energy to power a desalination plant in the North of Gran Canaria, concluding that it could be a feasible solution both from a socioeconomic and from an environmental point of view. Some prototype desalination plants indeed do already exist that are partially or totally powered by renewables (e.g. Cipollina et al., 2014; Rosales-Asensio et al., 2019).

3. Wave energy assessment

This Section analyses the available wave energy and the potential power production of a WEC in the waters of Tenerife. In Sub-section 3.1 the wave database is described, a suitable area for the installation is selected and the wave climate at the location is outlined. In Sub-section 3.2, the available wave power is calculated on an annual, seasonal and monthly basis. Finally, in Sub-section

3.3 the most suitable WEC is selected for the installation and the energy production is estimated for a typical year on a seasonal and monthly basis.

3.1 Typical wave climate

The detailed analysis of the wave energy potential of Tenerife Island can be performed based on 61 years of hourly wave data. The dataset covers the period 4 January 1958 - 31 December 2018 at the SIMAR point 1016015, located North-East off the coast of Tenerife island (28°45'N, 16°00'W), see Figure 1 and Figure 2. SIMAR dataset consists of hourly series of wave parameters (significant wave heights H_s, peak periods T_p and wave direction) derived from numerical modelling instead from direct measurements. This dataset, which offers information from 1958 to the present, has been developed by the Spanish governmental agency Puertos Del Estado, that is responsible for implementing the government's port policy, with the purpose of providing longer and daily updated time series of climate parameters. Two models were used to generate the wave fields: WAM and WAVEWATCH III (WW3), driven by the wind field data from the model provided by AEMET (i.e. the Spanish national agency of meteorology). The first two are third-generation spectral models that solve the energy balance equation without making assumptions about the wave spectrum. The models have been validated with measured data from buoys and satellite data by many authors (e.g. Goncalves et al., 2014, for the Isle of Gran Canaria and Silva et al., 2015, for the Iberian Peninsula).

Among the points of the SIMAR wave dataset situated around the Island of Tenerife, the selected point is the most energetic one and is also located in a suitable area (Veigas and Iglesias, 2013), since the Northern part of the island is not a tourist area, it is not an MPA (see Section 2.1) and it is far away from nautical trade routes (World seaports catalogue). However, Veigas and Iglesias (2013) excluded the point from their analysis because of the extreme water depth: in fact, it is located outside the continental shelf, approximately 22 km off the coast, at a depth of almost 3000 m. However, according to Gongalves et al. (2020), there is not such a great variation of the annual average wave power in this area, being it always in the range 16-18 kW/m. Therefore, in this analysis, the SIMAR point 1016015 dataset was considered in order to assess the wave climate, although the location for the WEC will be much closer to the shore, on the continental shelf, where the slope gradient is less than 1° (Llanes et al., 2003). In particular, the chosen location is about 4 km off the coast and 20 km from the port of Santa Cruz, at a depth of about 50 m (Figure 2).

For the purpose of this analysis, the direction intervals 0°-40° and 300°-360° were selected, being the more significant for energy generation, as the corresponding fetch is almost unlimited. The probability of occurrence for each combination of wave directions and wave heights is reported in Table 1. An example of the wave roses is reported in Figure 3 for a typical year. The H_s – direction matrix and the wave roses indicate that most of the waves come from NNE and N directions (0°-30°N and 350°-360°N) but the highest and most energetic waves come from NW and NNW directions (310°-330°N). By grouping all the selected data based on significant wave heights H_s and peak periods T_p, the most common wave conditions were identified in Table 2. The wave states characterized by H_s in the range 1-2 m and T_p in the range 7-8.5 s have the highest probability of occurrence. Moreover, the waves with $T_p > 9$ s are rather frequent and are associated with the highest values of available wave power.

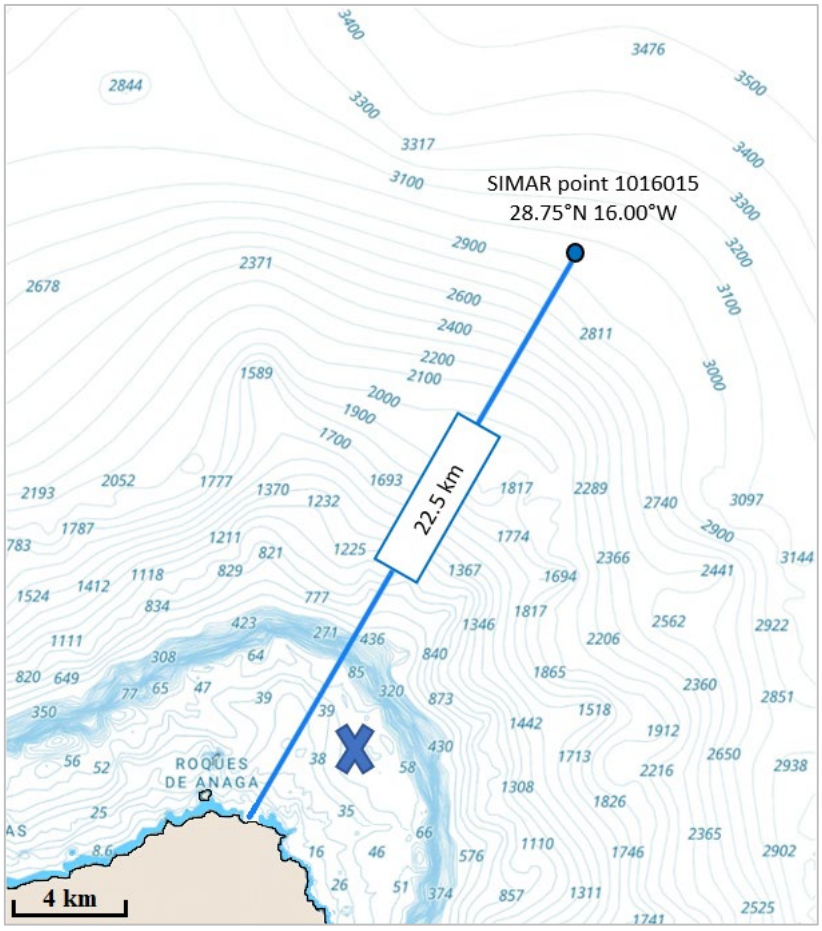

Figure 2. Bathymetry of the sea floor in the North-Eastern area off the coast of Tenerife, between the SIMAR point 1016015 (28°45'N, 16°00'W) and the shoreline. The blue cross indicates the possible area for the WEC installation.

Table 1. Probability of occurrence (%) for each significant wave height (m) and direction (°N) calculated over 61 years (1958-2018).

Hs/Dir	0°-10°	10°-20°	20°-30°	30°-40°	300°-310°	310°-320°	320°-330°	330°-340°	340°-350°	350°-360°	Σ
0-0.5	0.03%	0.02%	0.01%	0.00%	0.00%	0.02%	0.03%	0.03%	0.02%	0.03%	0.19%
0.5-1	1.58%	1.43%	0.82%	0.37%	0.28%	0.40%	0.76%	0.90%	1.04%	1.17%	8.74%
1-1.5	5.01%	5.23%	3.25%	1.47%	0.87%	1.38%	1.98%	2.30%	2.64%	3.33%	27.46%
1.5-2	4.05%	5.51%	4.61%	2.23%	1.12%	1.64%	2.07%	2.24%	2.48%	2.79%	28.74%
2-2.5	1.99%	2.91%	3.34%	1.80%	0.87%	1.11%	1.41%	1.56%	1.58%	1.63%	18.20%
2.5-3	0.81%	1.24%	1.50%	0.98%	0.55%	0.75%	0.91%	0.89%	0.85%	0.83%	9.31%
3-3.5	0.33%	0.40%	0.67%	0.42%	0.31%	0.43%	0.51%	0.49%	0.41%	0.36%	4.34%
3.5-4	0.11%	0.12%	0.21%	0.23%	0.16%	0.19%	0.22%	0.22%	0.17%	0.14%	1.78%
4-4.5	0.05%	0.04%	0.04%	0.05%	0.09%	0.10%	0.12%	0.10%	0.05%	0.04%	0.68%
4.5-5	0.02%	0.01%	0.02%	0.02%	0.04%	0.05%	0.06%	0.05%	0.02%	0.02%	0.32%
5-5.5	0.01%	0.00%	0.00%	0.01%	0.02%	0.02%	0.03%	0.01%	0.01%	0.01%	0.13%
5.5-6	0.00%	0.00%	0.00%	0.00%	0.01%	0.01%	0.01%	0.01%	0.00%	0.00%	0.05%
6-6.5	0.00%	0.00%	0.00%	0.00%	0.00%	0.01%	0.00%	0.00%	0.00%	0.00%	0.03%
6.5-7	0.00%	0.00%	0.00%	0.00%	0.00%	0.01%	0.00%	0.00%	0.00%	0.00%	0.01%
7-7.5	0.00%	0.00%	0.00%	0.00%	0.00%	0.00%	0.00%	0.00%	0.00%	0.00%	0.00%
7.5-8	0.00%	0.00%	0.00%	0.00%	0.00%	0.00%	0.00%	0.00%	0.00%	0.00%	0.00%
8-8.5	0.00%	0.00%	0.00%	0.00%	0.00%	0.00%	0.00%	0.00%	0.00%	0.00%	0.00%
8.5-9	0.00%	0.00%	0.00%	0.00%	0.00%	0.00%	0.00%	0.00%	0.00%	0.00%	0.00%
Σ	13.99%	16.93%	14.47%	7.59%	4.34%	6.14%	8.11%	8.81%	9.28%	10.34%	100%

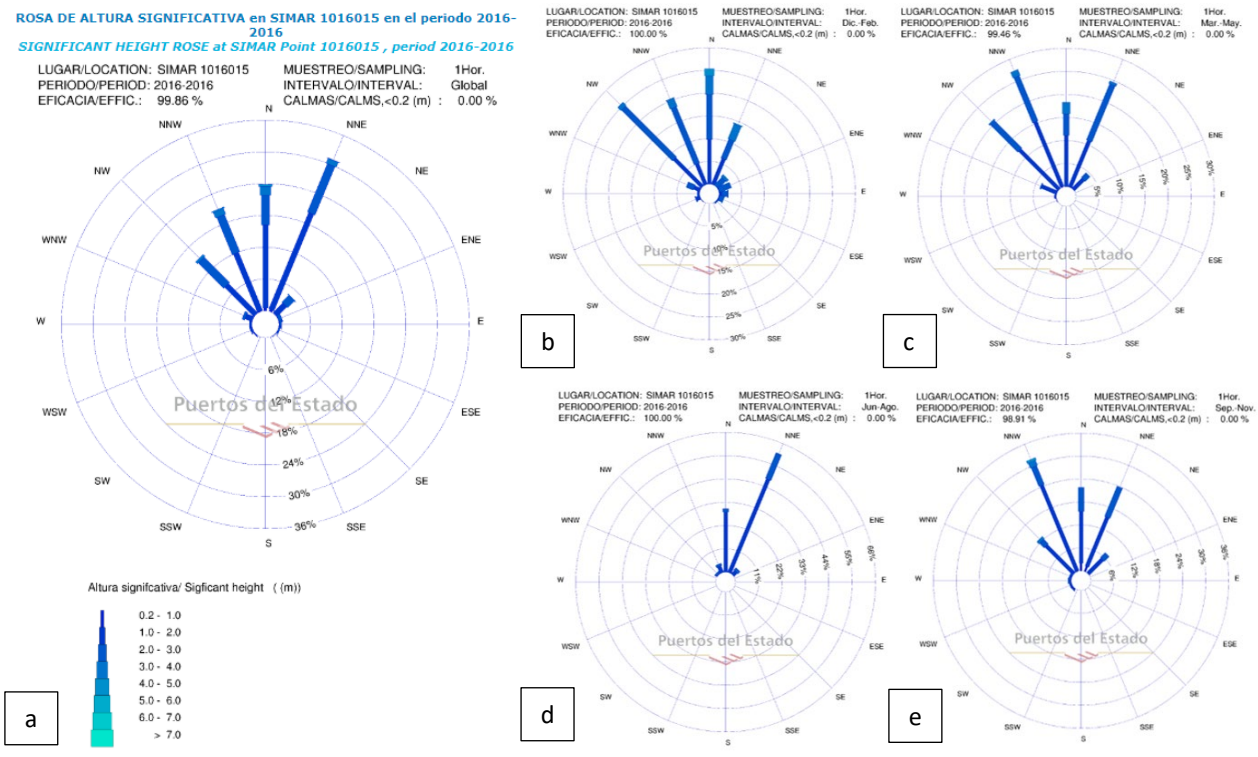

Figure 3. Wave roses for year 2016 (Puertos del Estado, Gobierno de Espana). a) Full year. b) Winter. c) Spring. d) Summer. e) Autumn.

Table 2. Probability of occurrence (%) for each combination of significant wave height (m) and peak period (s) calculated over 61 years (1958-2018).

Hs/Tp	2.5	3	3.5	4	4.5	5	5.5	6	6.5	7	7.5	8	8.5	9	9.5	10	10.5	11	11.5	12	12.5	13	13.5	14	14.5	15	15.5	16	16.5	17	17.5	18	18.5	19	19.5	20	20.5	21	21.5	∑
0.5	0.0%	0.0%	0.0%	0.0%	0.0%	0.0%	0.1%	0.2%	0.2%	0.3%	0.2%	0.1%	0.2%	0.1%	0.1%	0.1%	0.1%	0.1%	0.0%	0.0%	0.0%	0.0%	0.0%	0.0%	0.0%	0.0%	0.0%	0.0%	0.0%	0.0%	0.0%	0.0%	0.0%	0.0%	0.0%	0.0%	0.0%	0.0%	0.0%	2.0%
1	0.0%	0.0%	0.0%	0.0%	0.1%	0.3%	0.6%	1.2%	1.4%	1.7%	1.9%	1.8%	2.3%	1.6%	1.5%	1.5%	0.7%	1.0%	0.4%	0.4%	0.3%	0.1%	0.2%	0.1%	0.1%	0.0%	0.0%	0.0%	0.0%	0.0%	0.0%	0.0%	0.0%	0.0%	0.0%	0.0%	0.0%	0.0%	0.0%	19.3%
1.5	0.0%	0.0%	0.0%	0.0%	0.0%	0.1%	0.4%	1.3%	2.5%	3.0%	2.3%	1.9%	2.3%	1.9%	2.2%	2.7%	1.8%	2.6%	1.2%	1.4%	0.9%	0.4%	0.5%	0.2%	0.3%	0.1%	0.0%	0.1%	0.0%	0.0%	0.0%	0.0%	0.0%	0.0%	0.0%	0.0%	0.0%	0.0%	0.0%	30.4%
2	0.0%	0.0%	0.0%	0.0%	0.0%	0.0%	0.0%	0.2%	1.2%	2.7%	2.5%	1.8%	1.4%	0.8%	1.1%	1.4%	1.2%	2.3%	1.4%	1.8%	1.2%	0.7%	0.8%	0.3%	0.4%	0.2%	0.1%	0.1%	0.0%	0.0%	0.0%	0.0%	0.0%	0.0%	0.0%	0.0%	0.0%	0.0%	0.0%	23.9%
2.5	0.0%	0.0%	0.0%	0.0%	0.0%	0.0%	0.0%	0.0%	0.1%	0.5%	1.1%	1.6%	1.2%	0.5%	0.4%	0.5%	0.5%	1.0%	0.7%	1.1%	1.1%	0.6%	0.9%	0.3%	0.4%	0.2%	0.1%	0.1%	0.1%	0.0%	0.0%	0.0%	0.0%	0.0%	0.0%	0.0%	0.0%	0.0%	0.0%	13.2%
3	0.0%	0.0%	0.0%	0.0%	0.0%	0.0%	0.0%	0.0%	0.0%	0.1%	0.2%	0.5%	0.8%	0.3%	0.3%	0.2%	0.2%	0.4%	0.3%	0.5%	0.6%	0.4%	0.7%	0.2%	0.4%	0.2%	0.1%	0.1%	0.0%	0.0%	0.0%	0.0%	0.0%	0.0%	0.0%	0.0%	0.0%	0.0%	0.0%	6.5%
3.5	0.0%	0.0%	0.0%	0.0%	0.0%	0.0%	0.0%	0.0%	0.0%	0.0%	0.0%	0.1%	0.3%	0.2%	0.2%	0.1%	0.1%	0.1%	0.1%	0.2%	0.2%	0.2%	0.4%	0.1%	0.2%	0.1%	0.1%	0.1%	0.1%	0.0%	0.0%	0.0%	0.0%	0.0%	0.0%	0.0%	0.0%	0.0%	0.0%	2.8%
4	0.0%	0.0%	0.0%	0.0%	0.0%	0.0%	0.0%	0.0%	0.0%	0.0%	0.0%	0.0%	0.1%	0.1%	0.1%	0.0%	0.0%	0.0%	0.0%	0.0%	0.1%	0.1%	0.2%	0.1%	0.1%	0.1%	0.0%	0.1%	0.0%	0.0%	0.0%	0.0%	0.0%	0.0%	0.0%	0.0%	0.0%	0.0%	0.0%	1.2%
4.5	0.0%	0.0%	0.0%	0.0%	0.0%	0.0%	0.0%	0.0%	0.0%	0.0%	0.0%	0.0%	0.0%	0.0%	0.0%	0.0%	0.0%	0.0%	0.0%	0.0%	0.0%	0.0%	0.1%	0.0%	0.1%	0.0%	0.0%	0.0%	0.0%	0.0%	0.0%	0.0%	0.0%	0.0%	0.0%	0.0%	0.0%	0.0%	0.0%	0.4%
5	0.0%	0.0%	0.0%	0.0%	0.0%	0.0%	0.0%	0.0%	0.0%	0.0%	0.0%	0.0%	0.0%	0.0%	0.0%	0.0%	0.0%	0.0%	0.0%	0.0%	0.0%	0.0%	0.0%	0.0%	0.0%	0.0%	0.0%	0.0%	0.0%	0.0%	0.0%	0.0%	0.0%	0.0%	0.0%	0.0%	0.0%	0.0%	0.0%	0.2%
5.5	0.0%	0.0%	0.0%	0.0%	0.0%	0.0%	0.0%	0.0%	0.0%	0.0%	0.0%	0.0%	0.0%	0.0%	0.0%	0.0%	0.0%	0.0%	0.0%	0.0%	0.0%	0.0%	0.0%	0.0%	0.0%	0.0%	0.0%	0.0%	0.0%	0.0%	0.0%	0.0%	0.0%	0.0%	0.0%	0.0%	0.0%	0.0%	0.0%	0.1%
6	0.0%	0.0%	0.0%	0.0%	0.0%	0.0%	0.0%	0.0%	0.0%	0.0%	0.0%	0.0%	0.0%	0.0%	0.0%	0.0%	0.0%	0.0%	0.0%	0.0%	0.0%	0.0%	0.0%	0.0%	0.0%	0.0%	0.0%	0.0%	0.0%	0.0%	0.0%	0.0%	0.0%	0.0%	0.0%	0.0%	0.0%	0.0%	0.0%	0.0%
6.5	0.0%	0.0%	0.0%	0.0%	0.0%	0.0%	0.0%	0.0%	0.0%	0.0%	0.0%	0.0%	0.0%	0.0%	0.0%	0.0%	0.0%	0.0%	0.0%	0.0%	0.0%	0.0%	0.0%	0.0%	0.0%	0.0%	0.0%	0.0%	0.0%	0.0%	0.0%	0.0%	0.0%	0.0%	0.0%	0.0%	0.0%	0.0%	0.0%	0.0%
7	0.0%	0.0%	0.0%	0.0%	0.0%	0.0%	0.0%	0.0%	0.0%	0.0%	0.0%	0.0%	0.0%	0.0%	0.0%	0.0%	0.0%	0.0%	0.0%	0.0%	0.0%	0.0%	0.0%	0.0%	0.0%	0.0%	0.0%	0.0%	0.0%	0.0%	0.0%	0.0%	0.0%	0.0%	0.0%	0.0%	0.0%	0.0%	0.0%	0.0%
7.5	0.0%	0.0%	0.0%	0.0%	0.0%	0.0%	0.0%	0.0%	0.0%	0.0%	0.0%	0.0%	0.0%	0.0%	0.0%	0.0%	0.0%	0.0%	0.0%	0.0%	0.0%	0.0%	0.0%	0.0%	0.0%	0.0%	0.0%	0.0%	0.0%	0.0%	0.0%	0.0%	0.0%	0.0%	0.0%	0.0%	0.0%	0.0%	0.0%	0.0%
8	0.0%	0.0%	0.0%	0.0%	0.0%	0.0%	0.0%	0.0%	0.0%	0.0%	0.0%	0.0%	0.0%	0.0%	0.0%	0.0%	0.0%	0.0%	0.0%	0.0%	0.0%	0.0%	0.0%	0.0%	0.0%	0.0%	0.0%	0.0%	0.0%	0.0%	0.0%	0.0%	0.0%	0.0%	0.0%	0.0%	0.0%	0.0%	0.0%	0.0%
∑	0.0%	0.0%	0.0%	0.0%	0.1%	0.4%	1.2%	2.9%	5.6%	8.2%	8.2%	7.8%	8.6%	5.5%	5.9%	6.6%	4.6%	7.7%	4.1%	5.5%	4.4%	2.5%	3.7%	1.3%	1.9%	1.1%	0.5%	0.6%	0.3%	0.1%	0.2%	0.1%	0.0%	0.0%	0.0%	0.0%	0.0%	0.0%	0.0%	100%

253 ### 3.2 Available wave power

254 The wave power can be obtained, for each wave condition, according to Eq. 1:

$$P_w = \frac{\rho g^2 H_s^2 T_e}{64\pi} \quad \text{Eq. 1}$$

255 where P_w is the wave power per unit of crest length (kW/m), T_e is the energetic period (assumed to
256 be $0.9T_p$), ρ is the water density (assumed to be 1.025 kg/m^3) and g is the gravitational acceleration.
257 These values of theoretical wave power, calculated for each wave condition, were multiplied by the
258 corresponding probability of occurrence to estimate the realistic available wave power *P*. The
259 average annual value of *P* over 61 years, is $P_{y,m}$ = 18.54 kW/m (see Table 3). In order to assess the
260 variability of *P* over the years, the same procedure was repeated for each year. The results, reported
261 in Figure 4, show that there are no significant variations over the years. In particular, *P* ranges from
262 a minimum of 11.86 kW/m (in 2009) to a maximum of 26.71 kW/m (in 2018), but the years in which
263 *P* exceeds 20 kW/m are rather rare, as well as the years in which *P* doesn't exceed 15 kW/m. The
264 available *P* was also calculated on a monthly and on a seasonal basis. The series of estimated
265 seasonal power data are graphically represented through their quartiles in Figure 5. On average,
266 29.39 kW/m are available during Winter (i.e. 59% more than $P_{y,m}$), 19.50 kW/m during Spring (5%
267 more than $P_{y,m}$), 16.04 kW/m during Autumn (13% less than $P_{y,m}$) and 10.44 during Summer (44%
268 less than $P_{y,m}$), with little variation over the years.

269 The column chart showing the variability of the monthly power for year 2016 is reported in Figure
270 6. Specifically, the year 2016 was selected as reference typical year over the last decade, considering
271 both the yearly available power (20.12 kW/m) and the seasonal power distribution (31.86 kW/m
272 during Winter, 21.34 kW/m during Spring, 17.19 kW/m during Autumn and 11.48 during Summer).
273 In fact, both the yearly average power and each seasonal average power are close to their respective
274 median value (see Figure 5) and the percentage difference between each seasonal value and the
275 yearly value is almost exactly equal to the corresponding average value over the observed 61 years
276 (in particular, 58% more than the annual average value during Winter, 6% more during Spring, 15%
277 less during Autumn and 43% less during Summer).

278

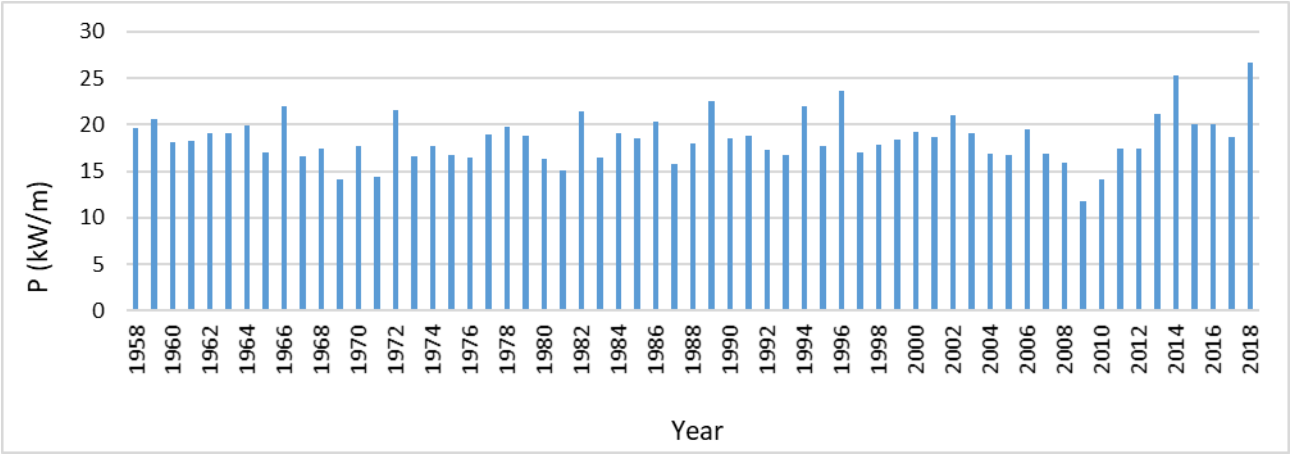

279

280 Figure 4. Average available wave power *P* calculated on an annual basis (kW/m).

Table 3. Wave power for each sea state considering the relative probability of occurrence (kW/m) calculated over 61 years (1958-2018).

Hs/Tp	2.5	3	3.5	4	4.5	5	5.5	6	6.5	7	7.5	8	8.5	9	9.5	10	10.5	11	11.5	12	12.5	13	13.5	14	14.5	15	15.5	16	16.5	17	17.5	18	18.5	19	19.5	20	20.5	21	21.5	∑
0.5	0.00	0.00	0.00	0.00	0.00	0.00	0.00	0.00	0.00	0.00	0.00	0.00	0.00	0.00	0.00	0.00	0.00	0.00	0.00	0.00	0.00	0.00	0.00	0.00	0.00	0.00	0.00	0.00	0.00	0.00	0.00	0.00	0.00	0.00	0.00	0.00	0.00	0.00	0.00	0.02
1	0.00	0.00	0.00	0.00	0.00	0.01	0.02	0.03	0.04	0.05	0.06	0.06	0.09	0.06	0.06	0.07	0.03	0.05	0.02	0.02	0.02	0.01	0.01	0.00	0.00	0.00	0.00	0.00	0.00	0.00	0.00	0.00	0.00	0.00	0.00	0.00	0.00	0.00	0.00	0.73
1.5	0.00	0.00	0.00	0.00	0.00	0.01	0.02	0.08	0.16	0.21	0.17	0.15	0.20	0.17	0.21	0.27	0.19	0.29	0.14	0.17	0.11	0.06	0.07	0.02	0.04	0.02	0.01	0.01	0.01	0.00	0.00	0.00	0.00	0.00	0.00	0.00	0.00	0.00	0.00	2.78
2	0.00	0.00	0.00	0.00	0.00	0.00	0.00	0.02	0.14	0.33	0.33	0.25	0.22	0.13	0.18	0.25	0.22	0.46	0.28	0.37	0.27	0.16	0.20	0.07	0.10	0.05	0.03	0.03	0.01	0.01	0.01	0.01	0.00	0.00	0.00	0.00	0.00	0.00	0.00	4.15
2.5	0.00	0.00	0.00	0.00	0.00	0.00	0.00	0.00	0.02	0.10	0.22	0.36	0.27	0.12	0.11	0.14	0.15	0.31	0.23	0.38	0.37	0.22	0.32	0.11	0.17	0.08	0.04	0.05	0.03	0.01	0.01	0.01	0.00	0.00	0.00	0.00	0.00	0.00	0.00	3.86
3	0.00	0.00	0.00	0.00	0.00	0.00	0.00	0.00	0.00	0.02	0.05	0.15	0.27	0.11	0.11	0.07	0.07	0.17	0.12	0.24	0.29	0.19	0.36	0.13	0.22	0.12	0.06	0.08	0.03	0.01	0.02	0.01	0.00	0.01	0.01	0.00	0.00	0.00	0.00	2.95
3.5	0.00	0.00	0.00	0.00	0.00	0.00	0.00	0.00	0.00	0.00	0.00	0.04	0.15	0.08	0.09	0.04	0.04	0.07	0.06	0.10	0.15	0.12	0.26	0.10	0.16	0.11	0.06	0.09	0.05	0.02	0.02	0.01	0.01	0.00	0.01	0.00	0.00	0.00	0.00	1.83
4	0.00	0.00	0.00	0.00	0.00	0.00	0.00	0.00	0.00	0.00	0.00	0.01	0.04	0.04	0.07	0.03	0.03	0.02	0.02	0.04	0.08	0.05	0.15	0.07	0.11	0.07	0.04	0.06	0.04	0.02	0.03	0.01	0.00	0.00	0.00	0.00	0.00	0.00	0.00	1.05
4.5	0.00	0.00	0.00	0.00	0.00	0.00	0.00	0.00	0.00	0.00	0.00	0.00	0.00	0.01	0.02	0.02	0.01	0.02	0.01	0.03	0.03	0.03	0.08	0.03	0.07	0.06	0.03	0.03	0.02	0.01	0.01	0.00	0.00	0.00	0.00	0.00	0.00	0.00	0.00	0.52
5	0.00	0.00	0.00	0.00	0.00	0.00	0.00	0.00	0.00	0.00	0.00	0.00	0.00	0.00	0.01	0.01	0.01	0.01	0.01	0.01	0.01	0.02	0.04	0.02	0.04	0.05	0.02	0.02	0.01	0.01	0.01	0.00	0.00	0.00	0.00	0.00	0.00	0.00	0.00	0.31
5.5	0.00	0.00	0.00	0.00	0.00	0.00	0.00	0.00	0.00	0.00	0.00	0.00	0.00	0.00	0.00	0.00	0.01	0.00	0.00	0.00	0.00	0.01	0.01	0.01	0.02	0.03	0.01	0.01	0.02	0.00	0.01	0.00	0.00	0.00	0.00	0.00	0.00	0.00	0.00	0.15
6	0.00	0.00	0.00	0.00	0.00	0.00	0.00	0.00	0.00	0.00	0.00	0.00	0.00	0.00	0.00	0.00	0.00	0.00	0.00	0.00	0.00	0.01	0.01	0.01	0.01	0.02	0.01	0.01	0.01	0.00	0.00	0.00	0.00	0.00	0.01	0.00	0.00	0.00	0.00	0.09
6.5	0.00	0.00	0.00	0.00	0.00	0.00	0.00	0.00	0.00	0.00	0.00	0.00	0.00	0.00	0.00	0.00	0.00	0.00	0.00	0.00	0.00	0.00	0.00	0.00	0.01	0.01	0.01	0.01	0.00	0.00	0.00	0.00	0.00	0.00	0.00	0.00	0.00	0.00	0.00	0.05
7	0.00	0.00	0.00	0.00	0.00	0.00	0.00	0.00	0.00	0.00	0.00	0.00	0.00	0.00	0.00	0.00	0.00	0.00	0.00	0.00	0.00	0.00	0.00	0.00	0.01	0.00	0.00	0.00	0.00	0.00	0.00	0.00	0.00	0.00	0.00	0.00	0.00	0.00	0.00	0.02
7.5	0.00	0.00	0.00	0.00	0.00	0.00	0.00	0.00	0.00	0.00	0.00	0.00	0.00	0.00	0.00	0.00	0.00	0.00	0.00	0.00	0.00	0.00	0.00	0.00	0.00	0.00	0.00	0.01	0.00	0.00	0.00	0.00	0.00	0.00	0.00	0.00	0.00	0.00	0.00	0.01
8	0.00	0.00	0.00	0.00	0.00	0.00	0.00	0.00	0.00	0.00	0.00	0.00	0.00	0.00	0.00	0.00	0.00	0.00	0.00	0.00	0.00	0.00	0.00	0.00	0.00	0.00	0.00	0.01	0.00	0.00	0.00	0.00	0.00	0.00	0.00	0.00	0.00	0.00	0.00	0.01
∑	0.00	0.00	0.00	0.00	0.00	0.01	0.04	0.14	0.37	0.72	0.85	1.02	1.23	0.73	0.87	0.91	0.77	1.41	0.88	1.36	1.34	0.87	1.51	0.57	0.96	0.63	0.32	0.41	0.24	0.09	0.12	0.06	0.02	0.02	0.03	0.01	0.00	0.01	0.01	18.54

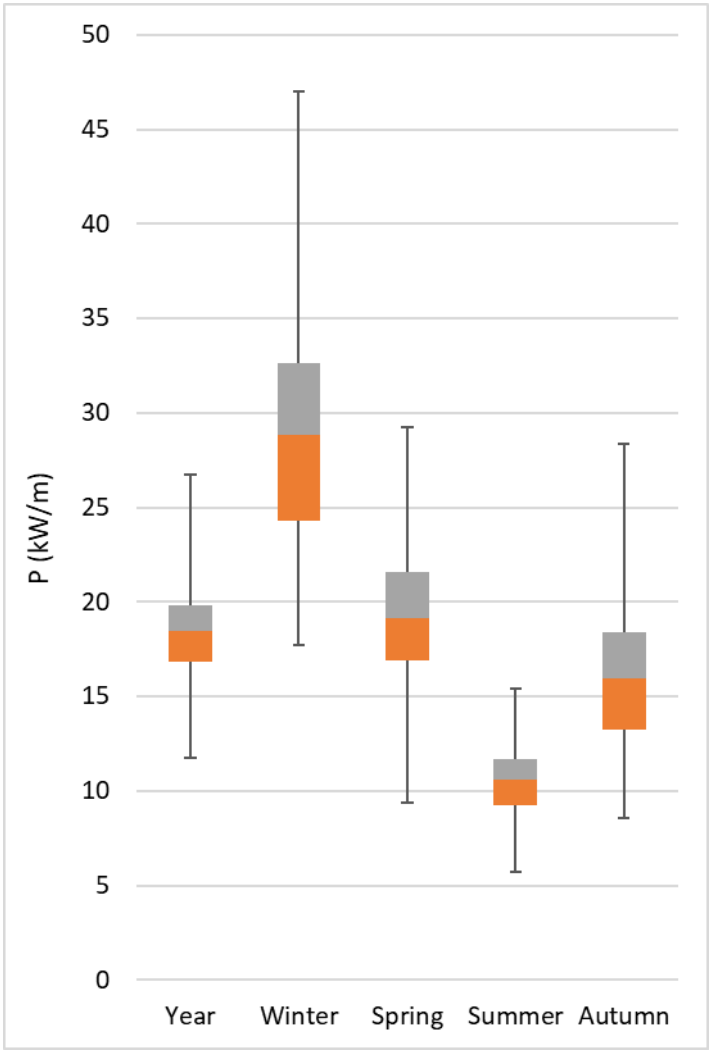

Figure 5. Box plots of the annual and seasonal available wave power *P* (years 1958-2018).

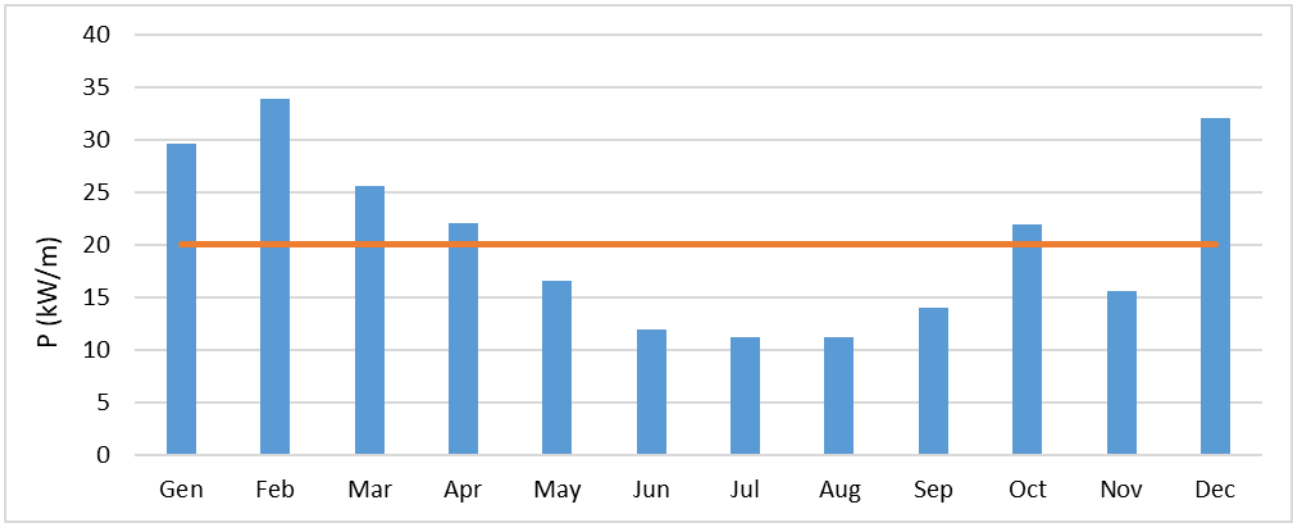

Figure 6. Available wave power *P* on a monthly basis for year 2016. The red line indicates the annual average wave power.

3.3 Wave energy harvesting

In the selection of the most suitable WEC for a particular location, there are many factors to be considered, such as: the distance from shore, the water depth, the visual and the environmental impact, besides the wave climate conditions. Moreover, the power matrix or power curve is freely available only for a few WECs, allowing for the preliminary estimation of the power production.

In the present case, being Tenerife a tourist island, only near-shore and offshore WECs have been considered, in order to minimize the visual impact. Furthermore, the Canaries are volcanic islands, which entails two important consequences: they are characterized by a steep sea bottom, thus great depths are reached close to the coast, and they can be subjected to earthquakes. For these reasons, only floating WECs were investigated.

With regard to the wave climate (Figure 3), most of the waves come from the Northern sector and the wave steepness is quite low for most of the time (Figure 7). Devices whose technology is based on the pitch, like DEXA (Zanuttigh et al., 2010; Martinelli & Zanuttigh, 2018) and Pelamis (Henderson, 2006; Yemm et al., 2012), have therefore to be excluded. On the contrary, long waves with low steepness are a favourable condition for overtopping devices and specifically for terminator devices, given the limited range of wave directionality.

Consequently, the Wave Dragon, WD hereinafter, was selected for the site. The WD (Kofoed et al., 2006; Eskilsson et al., 2014) is an overtopping device operating in the range 1-8 m of H_s and 4-14 s of T_p. Among the few devices whose potential production in the various sea states is published, WD is also the only one whose Company is still operating. The main features of WD and its power matrix are reported respectively in Table 4 and Table 5.

The WD was recently selected for possible applications in the Canary Islands by Goncalves et al. (2014, 2020), who compared its performance to the one of Pelamis and Aqua Buoy devices (Goncalves et al., 2014) and also to the one of Oceantec, Seabased and Wavebob (Goncalves et al., 2020), finding that the WD always showed the highest power output.

The output power at the examined site in Tenerife (SIMAR point 1016015) was calculated for the selected reference year, 2016 (see Sub-section 3.2), on an hourly, monthly and seasonal basis (Table 6). A yearly energy production of 13.2 GWh/y was obtained, in agreement with the previous studies. The series of estimated monthly performance and energy data are graphically represented in Figure 8 and in Figure 9 respectively. The WD is always operational during summer, since waves are

characterized by a lower amount of energy but they all fall within the operative range of the device. During winter, the WD operates approximately 80% of the time, because the longest and more energetic waves are beyond the operative range of the device. As a result, the output power over the months remains almost unchanged and it is thus equally distributed over the different seasons.

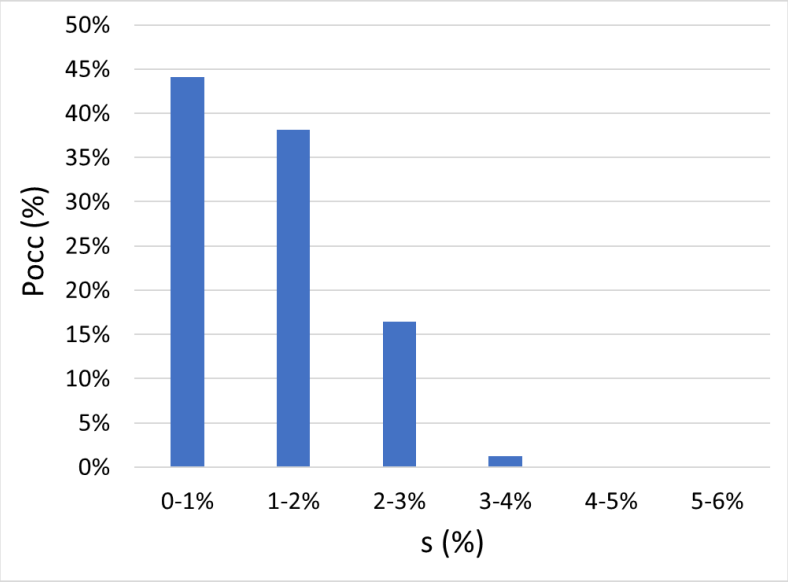

Figure 7. Probability of occurrence P_{occ} (%) of sea states characterized by different wave steepness s (%) for year 2016.

Table 4. Technical specifications for the business model of Wave Dragon optimized for a 24 kW/m typical wave climate (Kofoed et al., 2006; Sagaseta de Ilurdoz Cortadellas et al., 2011).

Typical wave power	24 kW/m
Total weight	22000 t
Main dimension (total length)	260 m
Secondary dimension (width)	150 m
Wave length of the reflector	126 m
Height	16 m
Reservoir	5000 m^3
Number of low-head Kaplan turbines	16
Permanent magnet generators	16x250 kW
Rated power	4 MW
Water depth	> 20 m

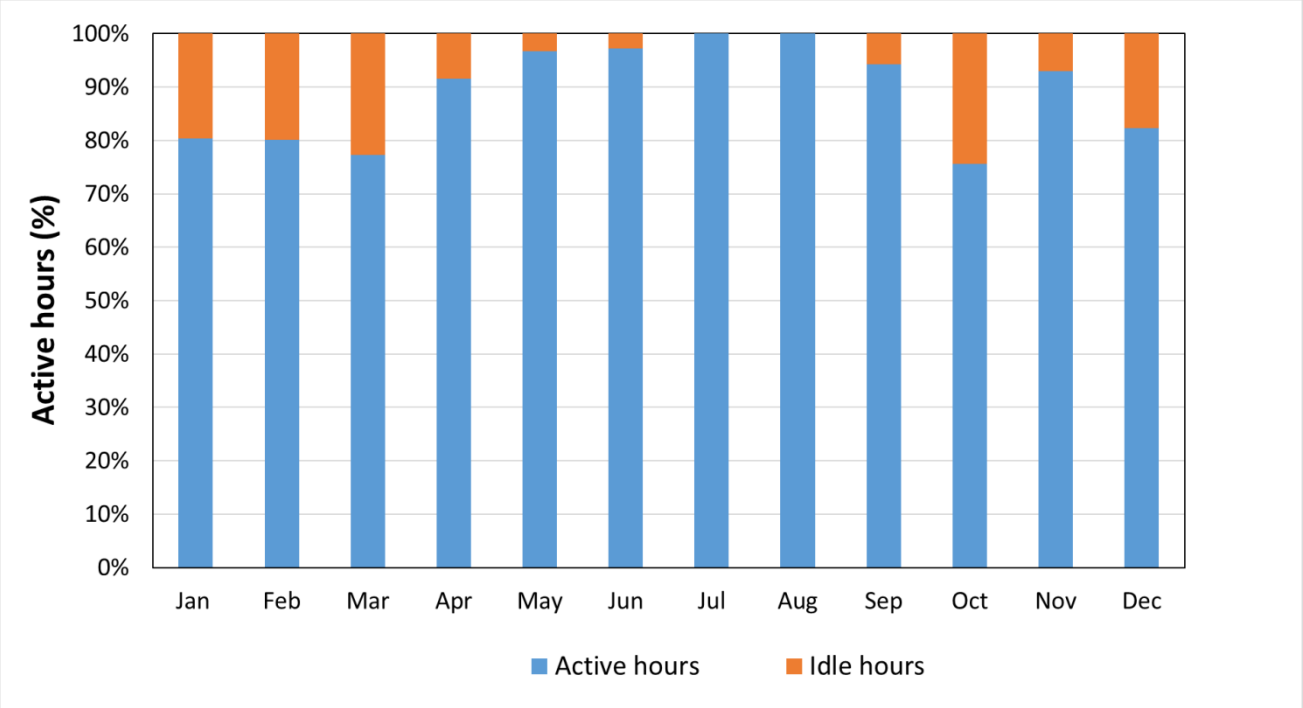

Figure 8. Monthly operating hours of the WD in Tenerife for year 2016.

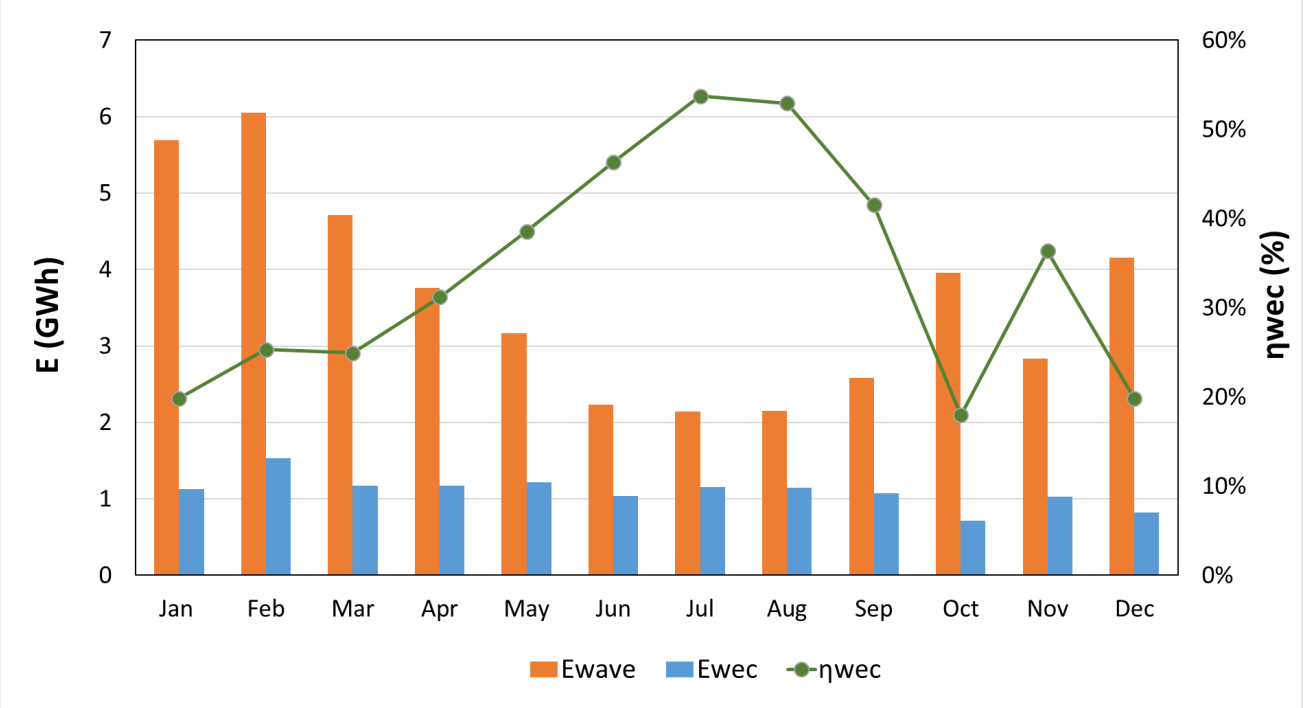

Figure 9. WD energy production per month (E_{wec}) in Tenerife for year 2016 and efficiency (η_{wec}) with respect to the monthly available energy (E_{wave}).

Table 5. Wave Dragon power matrix in kW (Carbon Trust, 2005).

Hs/Tp	4	4.5	5	5.5	6	6.5	7	7.5	8	8.5	9	9.5	10	10.5	11	11.5	12	12.5	13	13.5	14	∑
0.5	0	0	0	0	0	0	0	0	0	0	0	0	0	0	0	0	0	0	0	0	0	0
1	203	276	348	432	516	608	699	798	896	925	953	958	962	941	919	870	820	742	663	555	446	14530
1.5	412	448	485	617	750	899	1049	1212	1375	1433	1491	1509	1527	1502	1477	1404	1332	1209	1086	912	737	22866
2	621	621	621	802	983	1191	1398	1626	1853	1941	2029	2061	2092	2063	2034	1939	1844	1677	1509	1269	1028	31202
2.5	1123	1123	1123	1213	1304	1609	1914	2258	2602	2752	2903	2972	3041	3017	2993	2868	2743	2504	2266	1910	1555	45793
3	1624	1624	1624	1624	1624	2027	2430	2890	3350	3563	3776	3883	3989	3970	3951	3796	3641	3332	3022	2552	2082	60374
3.5	2581	2581	2581	2581	2581	2783	2984	3588	4191	4494	4796	4870	4945	4935	4926	4845	4765	4374	3983	3372	2761	79517
4	3538	3538	3538	3538	3538	3538	3538	4285	5032	5424	5816	5858	5900	5900	5900	5895	5889	5416	4943	4191	3439	98654
4.5	4719	4719	4719	4719	4719	4719	4719	5093	5466	5662	5858	5879	5900	5900	5900	5897	5895	5658	5422	4822	4222	110607
5	5900	5900	5900	5900	5900	5900	5900	5900	5900	5900	5900	5900	5900	5900	5900	5900	5900	5900	5900	5452	5004	122556
5.5	5900	5900	5900	5900	5900	5900	5900	5900	5900	5900	5900	5900	5900	5900	5900	5900	5900	5900	5900	5676	5452	123228
6	5900	5900	5900	5900	5900	5900	5900	5900	5900	5900	5900	5900	5900	5900	5900	5900	5900	5900	5900	5900	5900	123900
6.5	5900	5900	5900	5900	5900	5900	5900	5900	5900	5900	5900	5900	5900	5900	5900	5900	5900	5900	5900	5900	5900	123900
7	5900	5900	5900	5900	5900	5900	5900	5900	5900	5900	5900	5900	5900	5900	5900	5900	5900	5900	5900	5900	5900	123900
7.5	5900	5900	5900	5900	5900	5900	5900	5900	5900	5900	5900	5900	5900	5900	5900	5900	5900	5900	5900	5900	5900	123900
8	5900	5900	5900	5900	5900	5900	5900	5900	5900	5900	5900	5900	5900	5900	5900	5900	5900	5900	5900	5900	5900	123900
∑	56121	56230	56339	56826	57315	58674	60031	63050	66065	67494	68922	69290	69656	69528	69400	68814	68229	66212	64194	60211	56226	**1328827**

342 Table 6. Seasonal performance of Wave Dragon in Tenerife for year 2016.

Season	% active hours	Ewave (GWh)	Ewec (GWh)	η (%)
Winter	81%	15.89	3.48	22%
Spring	89%	11.64	3.57	31%
Summer	99%	6.53	3.33	51%
Autumn	88%	9.38	2.82	30%
Tot. year:	**89%**	**43.44**	**13.20**	**30.38%**

343

344 # 4. Solar Power Assessment

345 This Section analyses the available solar irradiation and the potential power production of a selected
346 PV panel at a chosen location close to Santa Cruz de Tenerife. The database used in the present
347 study is described in Sub-section 4.1, where the hypothetical location of the PV installation is also
348 identified, while the available solar irradiance is reported in Sub-section 4.2 in terms of annual and
349 seasonal average. In Sub-section 4.3, a commercial PV panel is selected and the power produced is
350 estimated for the typical year on a seasonal basis.

351 ## 4.1 Solar radiation dataset

352 Data about solar variables were retrieved from "Copernicus Climate Data Store" provided by the
353 European Centre for Medium-range Weather Forecasts, through the "ERA5" dataset that collects
354 worldwide reanalysis data (ECMWF, 2020). Reanalysis data are generated through a process of
355 "data assimilation": physical and meteorological models are integrated with measures of critical
356 variables performed on the whole globe (Parker, 2016). "ERA5" data are available for every hour
357 since 1979 and are discretized on a globe grid with a resolution of 0.25° x 0.25° sexagesimal degrees
358 (24.5 km and 27.8 km in latitude and longitude respectively). In the present case, the last two
359 decades of data (1999-2018) were chosen in order to check seasonal and yearly variations of the
360 solar irradiation on the area of interest.

361 Since Tenerife is a rather large island, several reticulate nodes of the "ERA5" dataset fall within its
362 borders or in close proximity (see Figure 1). The presence of the peak of Mount Teide should be
363 taken into account in the selection of the more appropriate grid point, since it is better to place the
364 PV installation in an area well exposed to the South. Indeed, existing solar farms are located at the
365 South East of Mount Teide, in Arico and Abona (Gobierno de Canarias, 2017; 2020a). According to
366 ITER (2016), in Santa Cruz only a 100 kW plant is present up to now.

Therefore, the industrial area between Santa Cruz de Tenerife and La Laguna was selected for the present analysis. The closest reticulate point for solar data acquisition is located at 28°50' N and 16°25' W (Figure 1). The necessary raw data extracted from the dataset for the evaluation of solar irradiation are: (i) the surface net solar irradiation H_h [J/m^2], (ii) the direct irradiation H_{bh} [J/m^2] and (iii) the ground albedo ρ [rad], all referred to a horizontal capturing surface (EMCWF, 2020).

4.2 Available solar irradiance

The total solar irradiation H [J/m^2] on a surface with any inclination and orientation can be evaluated from Eq. 2, according to the procedure reported by UNI 8477 (UNI Standards, 1983):

$$H = R\ H_h = (R_{dir} + R_{diff} + R_{refl})\ H_h \qquad \text{Eq. 2}$$

where H_h [J/m^2] is the surface net solar irradiation referred to a horizontal capturing surface, which consists of the direct irradiation H_{bh} [J/m^2] and the diffuse irradiation reaching a horizontal surface H_{dh} [J/m^2], while R is the percentage of solar radiation that hits the considered surface, which consists of the incident direct radiation (R_{dir}), the incident diffuse radiation (R_{diff}) and the radiation reflected from the ground (R_{refl}) depending on the ground albedo ρ [rad]. When R is lower than 1, more radiation is captured by horizontal surfaces than through inclined ones.

The available solar irradiation and irradiance are here examined in the general case of horizontal surfaces, while the inclination of the PV panels is optimized in Sub-section 4.3.

From the integration of H_h over the years, a yearly average solar irradiation of 6900 MJ/m^2 is obtained for horizontal surfaces.

The average hourly irradiance on a unit horizontal surface *PH* is therefore 219 W/m^2 on a 24-hours period and 404 W/m^2 if only sunlight hours are considered. A good yearly stability of irradiance is observed in the time span of 20 years (Figure 10): little variation of *PH* is registered throughout the two decades and no climate change effect is noticeable (Standard Deviation of 1.08% for both series).

The seasonality of solar irradiance is shown in Figure 11. As expected, full-day data show seasonal peaks in Spring and Summer, with an average irradiance of 278 and 263 W/m^2 respectively; conversely, Autumn and Winter present the minimum figures (153 and 180 W/m^2 respectively). The variations of seasonal mean values over the examined 20 years are minimal: the maximum percentage difference from the average seasonal value is observed during Autumn (3%). The

stability of both annual and seasonal average irradiance values allows for the selection of 2016 as a reference year, in line with the wave power analysis. In particular, in 2016 *PH* is 232 W/m^2 on a 24-hours period and 429 W/m^2 considering daylight hours only.

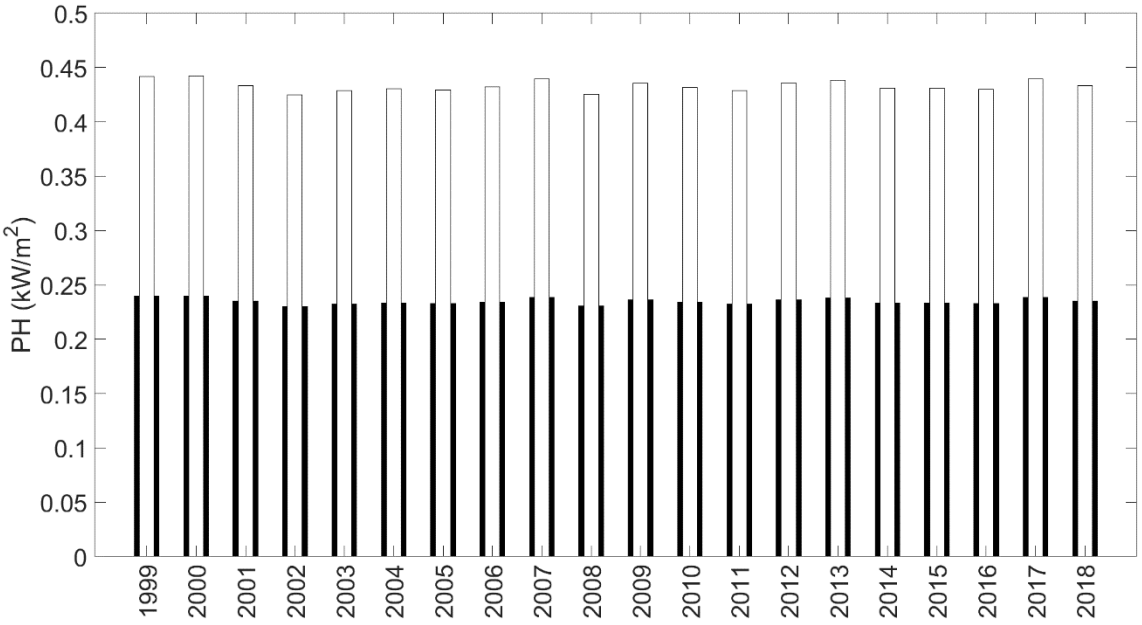

Figure 10. Average irradiance on a unit horizontal area (*PH*) in Tenerife from 1999 to 2008, considering 24 h (black bars) and the daylight hours only (white bars).

404

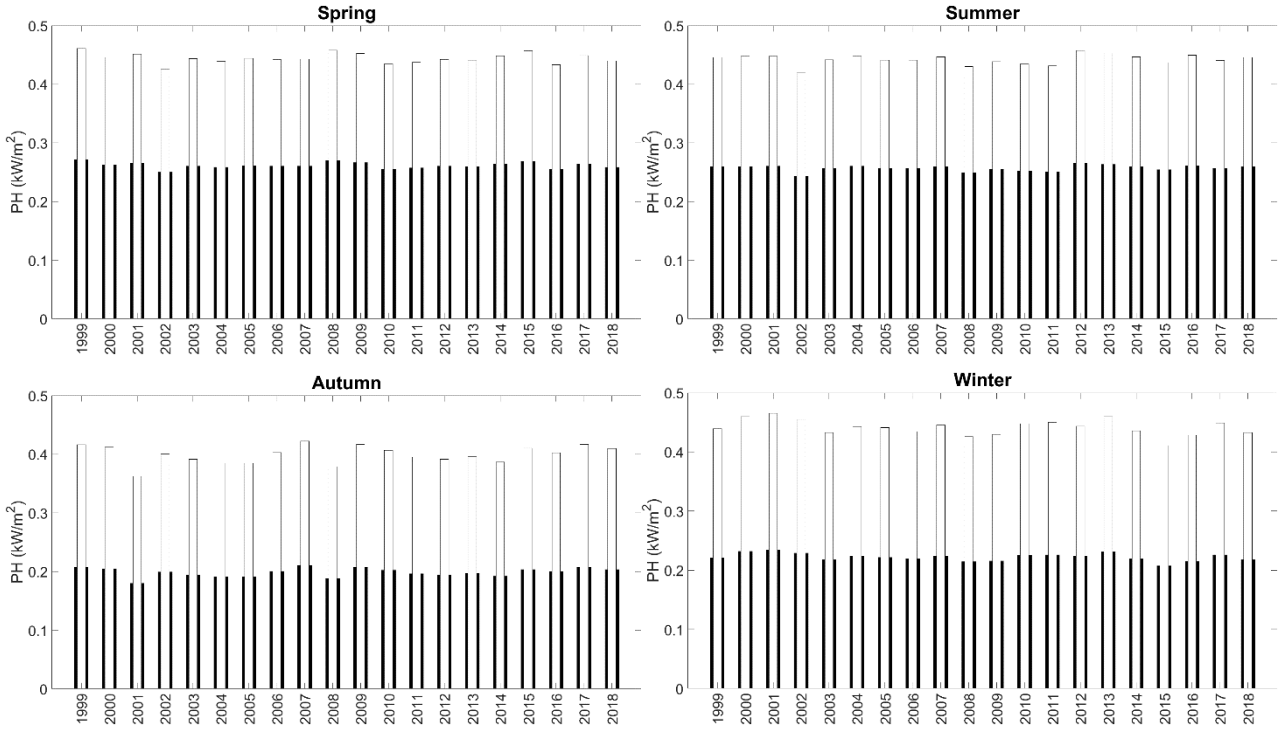

405

Figure 11. Seasonal averages of solar irradiance on a unit horizontal area (*PH*) considering 24 h (black bars) and the daylight hours only (white bars): a) Spring; b) Summer; c) Autumn; d) Winter.

406

407 ## 4.3 Solar energy harvesting

408 At present, photovoltaic systems are a well-developed technology in all their fixed configurations
409 (roof tops, grounded, over canals, in offshore platforms), presenting a wide variety of materials,
410 radiation-tracking designs, connecting modes, cooling systems (Khare, 2020).

411 Solar irradiation is differently valorised depending on the technology employed and on the exposure
412 and inclination of the panels (see Sub-section 4.2, Eq.2). Fixed-oriented panels were selected for the
413 present application and the exposure angles of the modules were optimised in order to maximise
414 the annual irradiation, H_{year}, for the selected reference year 2016. According to UNI 8477 (UNI
415 Standards, 1983) the optimum figures obtained for Azimuth and Inclination angles are respectively
416 0° (South exposition) and 23° with respect to the horizontal, leading to an increase of the average
417 irradiance *PH* in the reference year 2016 up to 244 W/m^2 on a 24-hours period and 450 W/m^2
418 considering the daylight hours only.

419 A medium-class panel was selected for the present application. Its main characteristics are reported
420 in Table 7.

421

Table 7. Technical characteristics of the selected commercial PV panel (Canadian Solar, 2020). W_p is the peak power, i.e. the maximum power produced by the panel.

Class of performance	Model name	Type	η_{PV} [%]	W_p/A [W/m^2]	W_p [W]	Weight [kg]	Cost [Euro]
Medium	CanadianSolar CS6K 270P	Poly-crystalline	16.8	164.9	270	18.2	170

The average hourly electric power produced in the *n*-th hour $P_{el,FV,n}$ [W] was derived from Eq. 3, according to the procedure proposed by UNI TS 11300-4 (Design of photovoltaic plants):

$$P_{el,FV,n} = \frac{PH_n}{I_{ref}} \; A_{PV} \; \eta_{PV} \; f_{PV} \qquad \text{Eq. 3}$$

where PH_n is the irradiance in the *n*-th hour [W/m^2]; I_{ref} is the reference instantaneous irradiance equal to 1 kW/m^2; A_{PV} [m^2] is the total area of the capturing surface; η_{PV} is the nominal efficiency considering the electric power production of the module with an instantaneous solar irradiance of 1 kW/m^2 at 25 °C (STC); f_{PV} is the system efficiency factor, also known as relative efficiency, considering the DC/AC conversion system, the irradiation variability and the operative temperature of the modules.

The seasonal averages of hourly electric power production for the selected PV panel and for the reference year 2016 are reported in Table 8. The seasonal variability of $P_{el,FV,n}$ is more pronounced than the seasonal values for the solar irradiance (reported in Sub-section 4.2), as the relative efficiency negatively affects the performance in periods with reduced *PH* levels. On the contrary, Spring and Summer present the maximum irradiance which boosts f_{PV} and, consequently, $P_{el,FV,n}$, overcoming the negative effect due to the increased module temperature.

Table 8. Seasonal averages and maxima for the hourly electric power $P_{el,FV,n}$ (W/m^2) produced by the selected medium-class panel in the reference year 2016.

	$P_{el,FV,n}$ - hourly average on full day	$P_{el,FV,n}$ - hourly average on daylight	Maximum $P_{el,FV,n}$
Spring	40	74	149
Summer	50	74	178
Autumn	30	69	168
Winter	26	58	103

443 The monthly power for the selected PV modules is shown in Figure 12. All over the year 2016, the
444 solar irradiation could have led to the production of 320.7 kWh/m^2 with the monthly trend shown
445 in Figure 13, where the gathered energy from the selected medium-performance PV system is
446 presented together with the average monthly system efficiencies.

447

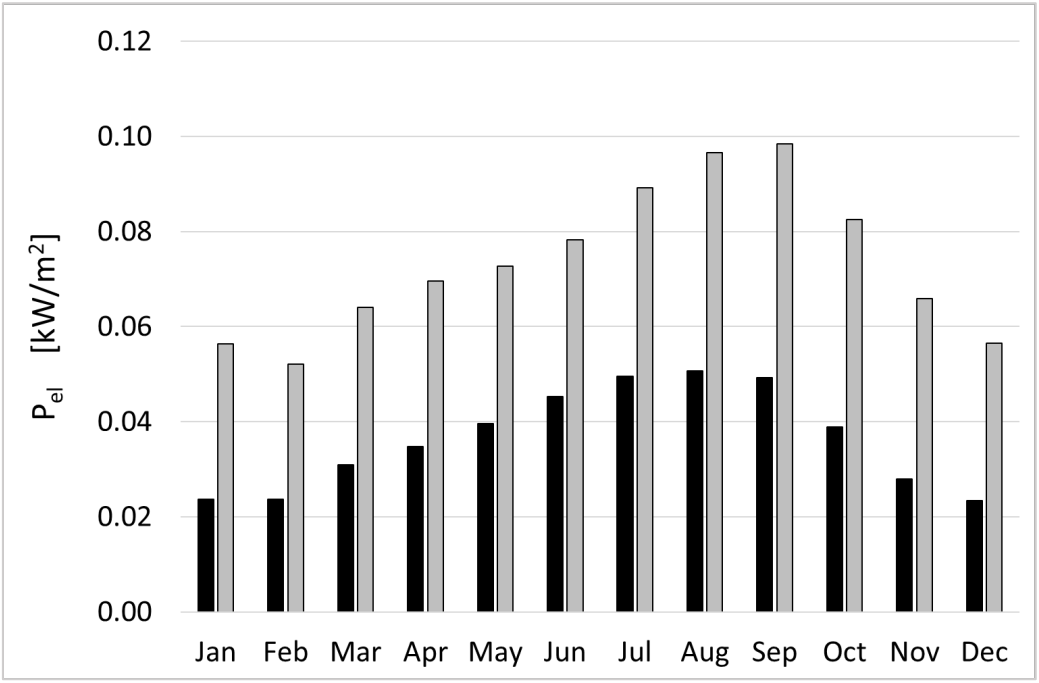

448

449 Figure 12. Monthly averages for the electric power (P_{el}) produced from the selected PV panel
450 during the reference year 2016 (in black whole day averages; in grey, daylight averages).

451

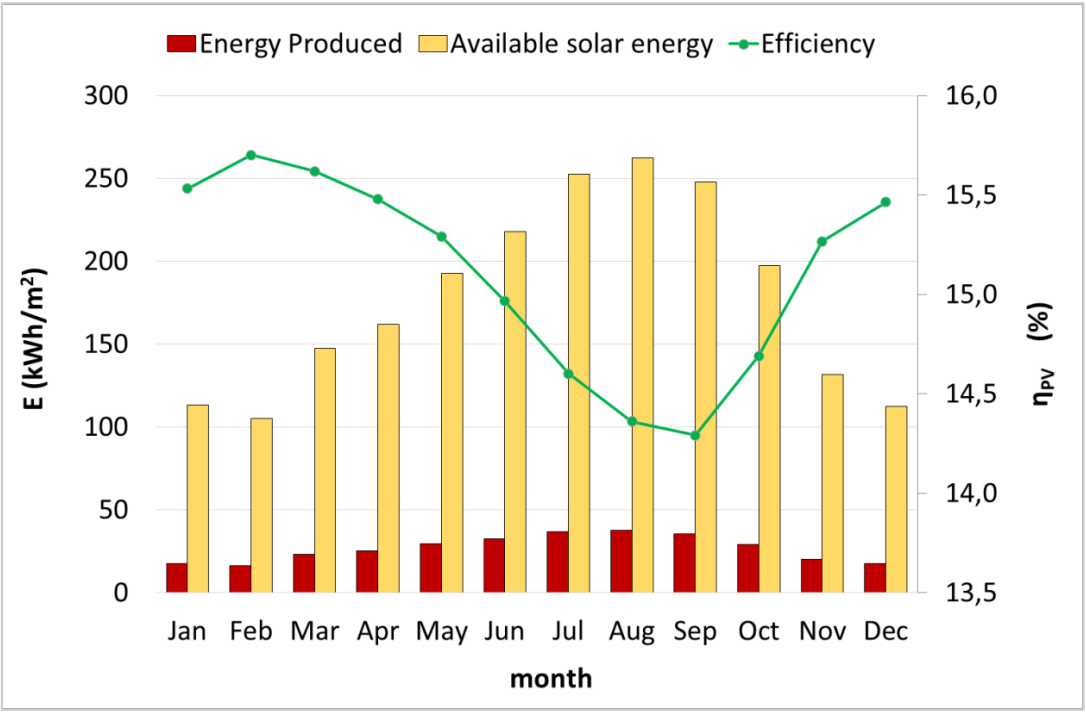

Figure 13. Comparison between the available solar irradiation and the energy produced per unit area by the selected medium-class panel in Tenerife in 2016. In the secondary axis, the efficiency of the PV panel (η_{PV}) is reported.

5. Design of the hybrid plant

This Section considers the use of wave and solar energy to supply a desalination facility. The characteristics of the desalinisation plant are defined in Sub-section 5.1. The additional components of the power supply system are reported in Sub-section 5.2. The features of the optimal mixing are identified in Sub-section 5.3.

5.1 Sizing of the onshore desalinization plant

The municipal marine water desalination plant of Santa Cruz de Tenerife, close to both the WEC and the solar plant potential installations, has a total capacity of 28000 m^3/day (EuropaPress, 2019), covering only the 67% of the water demand of Santa Cruz. In the present study, the combined RES installation is supposed to provide the power supply required by the enlargement of this plant, that would satisfy the entire water demand of the city, i.e. additional 14200 m^3/day of desalinated water. Furthermore, taking into account the population growth and the tourism increase in the last two decades (CityPopulation, 2020), the capacity of the RES-driven plant expansion is conservatively

increased to 16000 m^3/day. Considering an average water consumption of 0.16 m^3/day per-capita (Rosales-Asensio et al., 2020), the plant expansion would daily provide the water supply to 100'000 inhabitants, equivalent to almost half of Santa Cruz current population.

The selected desalination technology for the plant expansion is reverse osmosis (RO), due to its modularity and energetic convenience (Schallenberg-Rodríguez, et al. 2014). The consumption of a RO desalination plant is approximately 3 kWh/m^3 in recent applications (Rosales-Asensio et al., 2020).

Considering the selected capacity, the energy consumption for RO technology and the typical operating period of a desalination plant of 350 days/year (Rosales-Asensio et al., 2020), the annual consumption of the plant is 16.8 GWh/year, while the power threshold to be hourly satisfied by the integrated RES installation is 2 MW.

5.2 Components of the power supply system

In order to meet the energy requirements of the RO desalination plant in every condition, at least the following components have also to be installed in combination with the RES integrated system (Zanuttigh et al., 2021): an energy storage system; a generator set; a dummy load. Specifically, battery modules can be used for peak shaving, with the benefit of storing energy for the partial valley filling (Fathima and Palanisamy, 2018), whereas a fuel back-up system can assure the constant power threshold supply in every RES production condition, including the plant transients and start-ups (Verdolini et al., 2018). A dummy load, in the form of an electric resistance pack, should also be included to dissipate the power exceedance and stabilize the power performance of the integrated system (Zanuttigh et al., 2021). The detailed design of the electrical power system is out of the scope of this paper (the interested reader can refer to Zanuttigh et al., 2021), therefore, after focusing on the RES integration, only a rough sizing of the back-up system will follow. In particular, a low-duty simple-cycle gas turbine will be considered, due to its high flexibility and its high speed in the transients for power modulation (Gonzalez-Salazar et al., 2018).

5.3 Assessment of the RES optimal mixing

The main objective of this Section is the selection of most effective combination of the examined RES. The optimal RES mix is hereby designed to maximise the time during which the desalination duties are satisfied by RES only (indicated as t_{RES} hereinafter), given as a percentage with respect to

the total number of hours in a year. Simulations of possible mixing were performed by varying the number of wave energy converters as well as the available area for PV panels.

The RES functioning time is plotted as a function of the PV-panels area and of the number of WECs in Figure 14.

Once the power target is set, the number of WECs mainly drives t_{RES}, given their long operation time even as single resource. The solar park extends the power generation when the WECs are not operating and contributes to easily achieve the maximum t_{RES}, thanks to its modularity.

Specifically, a single WEC combined with the maximum considered PV-panels area would satisfy the power request for the 56% of the year only, while the installation of 2 WECs without PV-panels would increase t_{RES} to 77%. In this latter case, the combination of 2 WECs with the maximum area of the PV-panels boosts t_{RES} towards the asymptotic value of 88%. A good compromise is reached with 2 WECs and a PV-panels area between 30'000 and 40'000 m^2, assuring t_{RES} = 85%. Thus, the back-up system would be needed for the 15% of the plant operating time only.

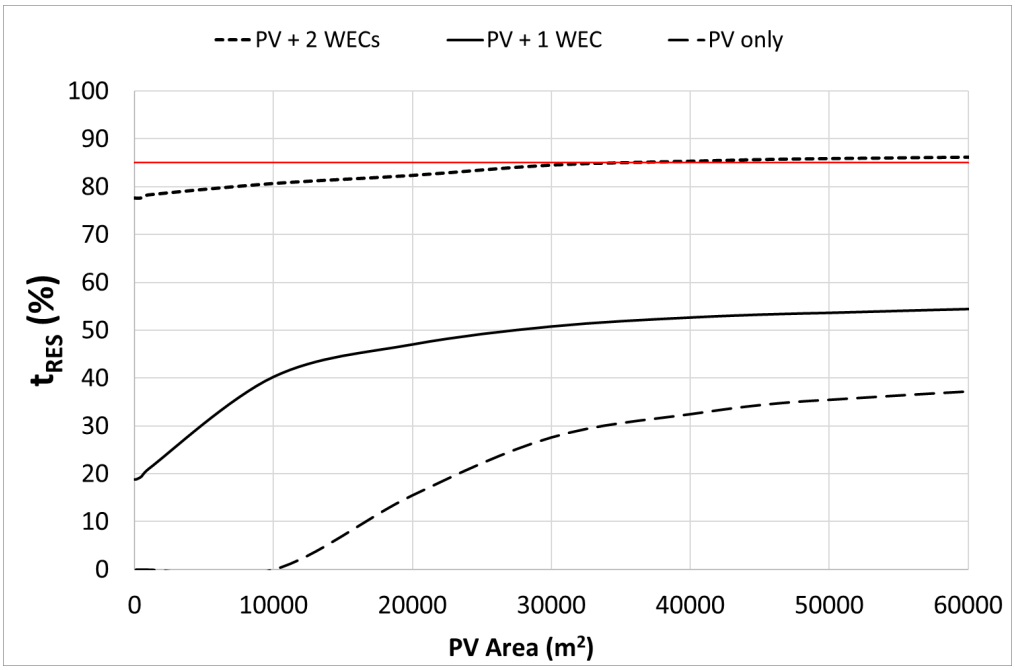

Figure 14. RES functioning time (t_{RES}) of the integrated system with variation of PV area and WECs number for a 2 MW desalination plant.

In summary, the optimal RES mixing is obtained by means of 2 WECs and a PV-panels area of 35'000 m^2. This combination (Figure 15):

- gives a high value of t_{RES}, equal to 85% (i.e. plant operating for the 85% of the year) and therefore reduces to 15% the Lack of Supply time t_{LS}, i.e. the percentage of production time in which the energy request is not satisfied by RES;
- ensures the Simultaneous Operation of the two RES plants for the 49% of t_{RES} (i.e. the 42% of the year); during this time, t_{SO} hereinafter, there is a good balance of the contribution of the two RES, because the WECs and the PV-panels contribute for the 59% and 41% respectively to the energy production during t_{SO};
- covers the energy needs during Non-Simultaneous Operation t_{NSO} (i.e. the remaining 51% of t_{RES} and therefore the 43% of the year) mostly by WECs (91% of t_{NSO}).

The main parameters and the production of the single RES installations and of the integrated RES plant are compared in Table 9.

As mentioned above, a back-up system is also introduced to cover t_{LS} (see Sub-section 5.2). The main operating parameters are reported in Table 10, where the nominal power is the maximum power requested in the present case study and the annual energy is the electrical energy to be produced by means of Natural Gas (NG) combustion. An average conversion performance of 35 % is considered (Ipieca, 2014) for the economic analysis in the next Section 6.

This procedure for optimal RES mixing is not site-specific and can be applied to combine different RES and to different loads. It requires as inputs:

- the hourly series of available power from RES;
- the production curve of the selected devices;
- the hourly power supply required by the additional activity or the characteristics of the connection to the power grid.

In the present application, a constant power threshold was assumed for the RO desalination plant. However, in many practical applications (e.g. fish farming or microalgae production), the energy requirements can be variable at different timescales: hourly, daily, or seasonally. Even in this case, being the criterion of the maximization of RES functioning time generally valid, the proposed methodology is applicable, as long as the variability of the energy demand is also known at hourly

level. Finally, all the energy losses were neglected, in particular the ones due to wave energy transfer to shore.

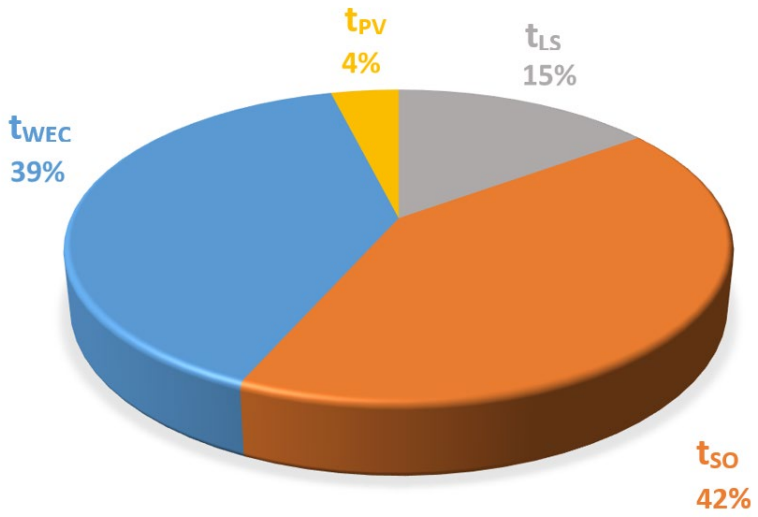

Figure 15. Simultaneous (t_{SO}) and Non-Simultaneous ($t_{NSO} = t_{WEC} + t_{PV}$, being t_{WEC} and t_{PV} respectively the operating time of WECs and of PV panels) operating times of the integrated plant over the year. Total year = $t_{LS} + t_{RES}$; $t_{RES} = t_{SO} + t_{NSO} = t_{SO} + t_{WEC} + t_{PV}$, where t_{RES} and t_{LS} are respectively the RES total operating time and the residual time of the year.

Table 9. Operating parameters of the integrated RES installation compared with the single RES installations supplying a 2MW desalination capacity.

	Wave Farm (2 WECs)	**Solar Park** (35'000 m^2)	**Integrated RES**
***t_{LS}* %**	17.2	69.7	15
***t_{RES}* %**	82.8	30.3	85
Nominal Power [kW]	11'900	5'770	17'670
Yearly Average Power [kW]	3'012	1'276	4'288
Yearly Energy Produced [GWh]	26.4	11.22	37.6
Energy of the peaks [GWh]	11.6	4.39	21.9
Energy of the valleys [GWh]	2.8	10.74	1.8
Max Power Missing [kW]	2'000	2'000	2'000
Max Surplus Power [kW]	9'800	4'235	12'984

559 Table 10. Back-up system performance and operating parameters.

Parameter	Value
Nominal Power (MW)	2
Annual Energy requested (MWh/y)	1818
EFLH - Equivalent Full Load Hours (h/y)	909
Average efficiency – based on LHV (%)	35
Annual Input Fuel Energy – based on HHV (MWh/y)	5771

560

561 # 6. Economics of the hybrid plant

562 The aim of this Section is to assess the economic performance of the hybrid plant. The economic
563 indicators considered in the analysis are defined in Sub-section 6.1. Costs of solar and wave energy
564 installations and of the backup system are evaluated in Sub-sections 6.2, 6.3 and 6.4 respectively.
565 The economic balance is reported in Sub-section 6.5.

566 ## 6.1 Economic indicators

567 The economic assessment of the integration of wave and solar energy is carried out for the typical
568 year 2016 by assuming the following economic indicators: the Levelized Cost of Energy (*LCOE*), the
569 Net Present Value (*NPV*) and the Payback Period (*PBP*).

570 The *LCOE* enables the direct comparison among energies derived from different sources and it
571 includes the lifetime of each installation (Segurado, Costa and Duić, 2018). The *LCOE* is determined
572 as follows:

$$LCOE = \frac{I_0 + \sum_{t=0}^{n} \frac{F_t + V_t}{(1+r)^t}}{\sum_{t=0}^{n} \frac{E_t}{(1+r)^t}} \quad \text{Eq. 4}$$

573 where r is the discount rate over the n years of the project, which takes into account the variation
574 of money value in time; I_0 represents the capital expenditures (CAPEX), i.e. the initial investment
575 costs at t=0; the sum of F_t and V_t (the fixed and variable operating costs respectively) represent the
576 operational expenditures (OPEX), i.e. the annual Operation and Maintenance (O&M) costs; E_t is the
577 energy produced by the plant in the t-th period.

578 The *NPV* and the *PBP* are calculated according to Eqs. 5 and 6 respectively, (Lauer, 2008). The *NPV*
579 allows the estimation of the actual value generated by the investment during the considered

lifetime. It consists of the sum of all the discounted cash flows (CF_t) of the *t*-th year (i.e. the difference between annual revenue and OPEX) minus the value of the CAPEX, i.e. the initial investment cost (I_0):

$$NPV = \sum_{t=1}^{n} \frac{CF_t}{(1+r)^t} - I_0 \qquad \text{Eq. 5}$$

The *NPV* therefore represents the Cumulated Cash Flow (CCF) actualized by applying the factor r.

Otherwise, the *PBP* indicates the time at which the company starts getting profits according to undiscounted *CFs*, i.e., the time at which the undiscounted cash flow equals the initial investment:

$$PBP = \{t | \sum_{t=1}^{n} CF_t = I_0\} \qquad \text{Eq. 6}$$

No discount rate is considered for the *CFs* in the *PBP* calculation, providing more optimistic results than the *NPV* calculation.

In Sub-sections 6.2 and 6.3, the *LCOE* is determined for solar and wave energy respectively, to allow a direct comparison with the typical values of the two sources, while the *PBP* and the *NPV* for the hybrid system are reported in Sub-section 6.5.

6.2 Levelized Cost of Solar Energy

Table 11 reports the parameters and the unitary costs used for the economic evaluations of the solar plant considered. The system losses include those due to Balance of System (*BOS*) devices, i.e. inverters, DC cables and AC cables, and those due to dust, snow and other deposits potentially covering the capturing surfaces (Photovoltaic-software, 2019). The degradation rate over production considers the natural performance decay of the PV cells over the years (Photovoltaic-software, 2019).

The *BOS* costs include the initial labour expenses for the infrastructure, for the support and installation of PV modules, for the modules DC cabling, for the setting and purchase of all the required electricity devices for transformation and grid connection.

Operation and Management (O&M) annual expenses include the replacement of modules, inverters and components, the module cleaning and vegetation management, system inspection & monitoring, operation administration costs (Reuters Events-Renewables, 2019).

Overheads are estimated to be 20% of the sum of the CAPEX and of the OPEX in accordance with the common practice of projects financial analysis (Culson and Richardson, 2017).

The values of the CAPEX and OPEX for solar facilities strongly depend on the installed capacity, being the costs of land purchase, of the modules and of all the needed devices for power transmission proportional to the total number of the installed panels. The CAPEX and the OPEX of the considered solar plant amount to 6 M€ and 63 k€/year respectively. The LCOE over the 30-years lifetime is equal to approximately 44 €/MWh, that increases to 54 €/MWh for a 20-years project. Both results fall within the reported range for the PV technology power generation in Europe (Kost *et al.*, 2018; Jäger-Waldau, 2019; Margolis, Feldman and Boff, 2020).

Table 11. Parameters and unitary costs considered for the economic assessment of the solar farm.

Parameter		**Value**	**Reference**
Land needed for installation (m^2)		35'000	Present work
Number of reference PV panels		21'376	Present work
Considered lifetime (y)		30	(Fu, et al. 2018)
Discount rate for solar farms (%)		4	(Guaita-Pradas and Blasco-Ruiz, 2020)
System losses on generation (%)		15	(Photovoltaic-software, 2019)
Degradation rate over production (%)		0.5	(Four Peaks Technologies, 2019)
Cost item		**Value**	**Reference**
Land in Tenerife (€/m^2)		5.9	(Access to land, 2013)
Modules (€/panel)		170	(Canadian Solar, 2020)
Inverters (€/kWp)		42	(Agora Energiewende, 2015)
BOS costs	Infrastructure (€/kWp)	40	(Agora Energiewende, 2015)
	Mounting (€/kWp)	75	(Agora Energiewende, 2015)
	Installation (€/kWp)	50	(Agora Energiewende, 2015)
	DC cabling (€/kWp)	50	(Agora Energiewende, 2015)
	Transformers, switchgears, planning, documentation) (€/kWp)	60	(Agora Energiewende, 2015)
	Grid Connection (€/kWp)	60	(Agora Energiewende, 2015)
O&M yearly costs for fixed-tilt panels (€/kW/y)		11	(Reuters Events-Renewables, 2019)
Overhead on CAPEX + OPEX (%)		20	(Culson and Richardson, 2017)

6.3 Levelized Cost of Wave Energy

With regard to the feasibility study for the WD installation, reference is made to the COE calculation tool for wave energy converters developed by Fernandez-Chozas et al. (2014). In the present study, this tool is used to make a comparison between the installation of a single and a couple of WDs.

620 Table 12 shows all the tool required inputs, besides the WEC power matrix (Table 5) and the wave
621 climate (Table 2). The assumptions about the WEC performance characteristics and the specific cost
622 items are here summarised.

623 • The mooring weight is up-scaled from Sorensen et al. (2015).
624 • The default values are adopted for the power take-off (PTO) and for the generator efficiencies,
625 while the WEC availability and the WEC's own consumption are assumed to be 95% and 10 kW
626 respectively (Frigaard et al., 2016).
627 • As for the structure costs, the percentages of different materials with respect to the total structure
628 weight and the costs related to the access system and machine housing are derived from Sorensen
629 et al. (2015).
630 • The default values are adopted for the prices per ton of material and for the cost of development,
631 of installation, of the electrical connection and of the PTO. In particular, the total suggested price
632 of the power take-off system is cautiously considered to be proportional to the nominal power and
633 results to be the most important cost item.
634 • The suggested values for contingencies, operation and maintenance costs per year and site lease
635 and insurance costs per year are assumed.

636 The resulting annual electricity production of one WD in Table 12 is slightly lower than the one reported
637 in Table 6, due to the necessary simplification of the climate matrix in the tool and to the efficiencies
638 considered. The resulting CAPEX and OPEX are about 33 M€ and 2.4 M€/y respectively for the
639 installation of a single WD.

640 In the case of two WDs, the following assumptions are made.

641 • The dimensions, the weights and the power are doubled, while WEC performance remain the
642 same. Therefore, the annual production and the costs of the structure, of the moorings, of the PTO
643 system and of the electrical connection result to be double.
644 • The cost of installation, including assembly and transport, is in this case doubled, while the
645 expenditures relative to development, access system and platform and machine housing are
646 supposed to be the same, i.e. a single substation is supposed to serve both WDs and the
647 maintenance operation are supposed to take place at the same time.
648 • The contingencies, operation and maintenance costs per year and site lease and insurance costs
649 per year are supposed to be the same as for one single WD.

650

651 The CAPEX for two WDs is less than twice the CAPEX previously estimated for one WD (64.5 M€),
652 while the OPEX is the same, leading to a decrease of the LCOE. Actually, assuming a discount rate of
653 4%, the LCOE equals respectively 357 €/MWh for one WD and 261 €/MWh for two WDs in 20 years.
654 Both values fall within the current range 250-600 €/MWh of LCOE of WECs reported by Fernandez-
655 Chozas et al. (2014) and are indeed much closer to the lower limit.

656 Table 12. Application of the COE tool – WEC features, performance and costs

Number of WECs	**1**	**2**
Project data		
Project lifetime (years)	20	20
Development phase	4	4
WEC features		
Main dimension (m)	260	520
Secondary dimension (m)	150	300
Weight - structure (ton)	22’000	44’000
- Concrete (ton)	21’830.77	43’661.54
- Steel (ton)	169.23	338.46
Weight - mooring (ton)	7’897.44	15’794.87
Rated power (kW)	4’000	8’000
WEC performance		
PTO average efficiency	95%	95%
Generator average efficiency	90%	90%
WEC's own consumption (MWh/y)	87.6	175.2
WEC availability	95%	95%
Annual electricity production (GWh/y)	**12.33**	**24.66**
Costs		
Development (default value: 3% CAPEX)	868’223	868’223
Main material (concrete, 200€/ton)	4’366’153	8’732’307
Other material (steel, 3400 €/ton)	575’384	1’150’769
Access system and platform	20’000	20’000
Machine housing	50’000	50’000
Structure (materials + access system&platform + machine housing)	5’011’538	9’953’076
Total PTO (default value: rated power x 5000 €/kW)	20’000'000	40’000’000
Mooring system (300 €/ton)	2’369’230	4’738’461
Total installation (default value: 200'000 €)	200’000	400’000
Electrical connection (default value: rated power x 340 €/kW)	1’360’000	2’720’000
Total CAPEX before contingiencies (€)	**29’808’992**	**58’679’761**
Contingencies (default value: 10% of total investment)	2'980’899	5’867’976
Total CAPEX (€)	**3.28E+07**	**6.45E+07**
Operation and maintenance costs per year (default value: 6% CAPEX)	1’788’539	1’788’539
Site lease and insurance (default value: 2% CAPEX)	596’179	596’179
Total OPEX (€/y)	**2.38E+06**	**2.38E+06**
Discount rate	4%	4%
LCOE (20 years, in €/MWh)	**357**	**261**

657

6.4 Cost of the back-up system

In Table 13, the cost items considered for the back-up system are reported. Medium values are assumed for the total CAPEX and for the standard O&M expenses of the back-up system. In addition, variable costs related to NG consumption are considered according to its current price in Spain.

Table 13. Economic parameters considered for the back-up system (cost items and prices).

Parameter	Value	Reference
CAPEX – Back-up system (€/kWp)	514	(U.S. Energy Information Administration, 2018)
O&M costs - Gas turbine (€/MWel/y)	0.3	(WADE, 2020)
NG price for businesses – Spain (€/kWht)	0.05	(GlobalPetrolPrices, 2020a)

6.5 Economic Balance

The economic balance is set by assuming that the total energy produced by the three sources (i.e. the wave farm, the solar park and the back-up system) is sold at the average electricity cost for businesses in Spain, that is 130 €/MWh (GlobalPetrolPrices, 2020b). The total energy is considered as the sum of the energy produced for the desalination plant and the exceeding energy production that would have been stored in the battery pack.

Extra revenues from the sale of produced wave energy are also considered by including government incentives for innovative power generation plants. In Spain, wave energy was rewarded with a Feed-In-Tariff (FIT) amounting to 86 €/MWh in 2014 (Fernandez-Chozas et al., 2014). Presently, this FIT has been replaced by different incentive schemes which don't comprise wave energy (Jimeno, 2019). Since energy policies are not mandatory and are often amended, different scenarios are investigated, in presence or absence of incentives on wave energy, as shown in Figure 16.

The *PBP* of the hybrid system without incentives is equal to 37 years, based on PV-panels first year performance, or to 39 years (Figure 16), considering deterioration over time and efficiency decrease of PV-panels. This *PBP* value is greater than the typical project lifetime of wave and solar installations but it is still lower than the desalination plant lifetime, which ranges from 20 to 60 years (Papapetrou et al., 2017). The *PBP* decreases to 17 years in case the Spanish FIT for wave energy is included.

The sensitivity of the profitability of the hybrid plant with respect to government incentives is performed by applying other FIT values provided in other countries (values at 2014). The *CCFs* of the project are evaluated including the incentives for wave energy of 367 and 600 €/MWh, as respectively supplied by the United Kingdom and Denmark (Fernández-Chozas et al, 2014). The

French support scheme is also applied as it proposes a middle-level remuneration, with an average yearly value of 139 €/MWh (Vidalic, 2019). In Figure 17 the *CCFs* are actualized taking into account the value of r = 4% equal to the case of the single RES plants. The parity point is reached when the actualized *CCF* (i.e., the *NPV*) is equal to zero. Although the *PBP* in the no-FIT scenario falls within the project lifetime, the *NPV* reveals a non-convenient investment even after 50 years. However, in case of FIT application, the *NPV* rises more rapidly with time and the parity point is reached within the project lifetime: the more the FIT is increased, the earlier the parity point is achieved, the higher the *NPV* results after a given period.

The economic assessment shows promising perspectives for future implementations of the hybrid plant, which can result rather profitable within 20 years when wave energy is remunerated through incentives of at least 140 €/MWh (see Table 14).

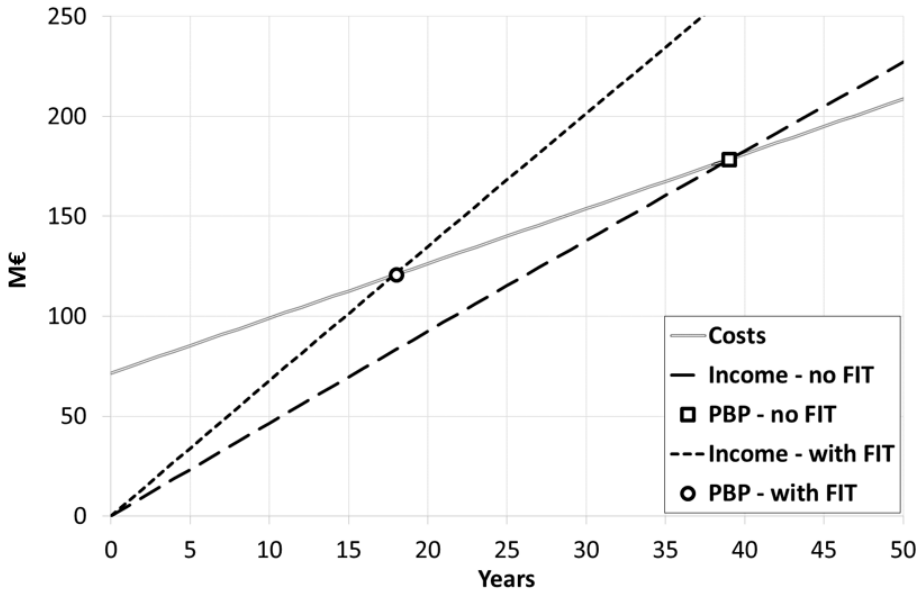

Figure 16. Cumulated costs (continuous line) and revenues of the hybrid power plant without incentives (dotted line) and with FIT= 86 €/MWh for wave energy (dashed line). Deterioration over time of PV-panels was taken into account in the calculations.

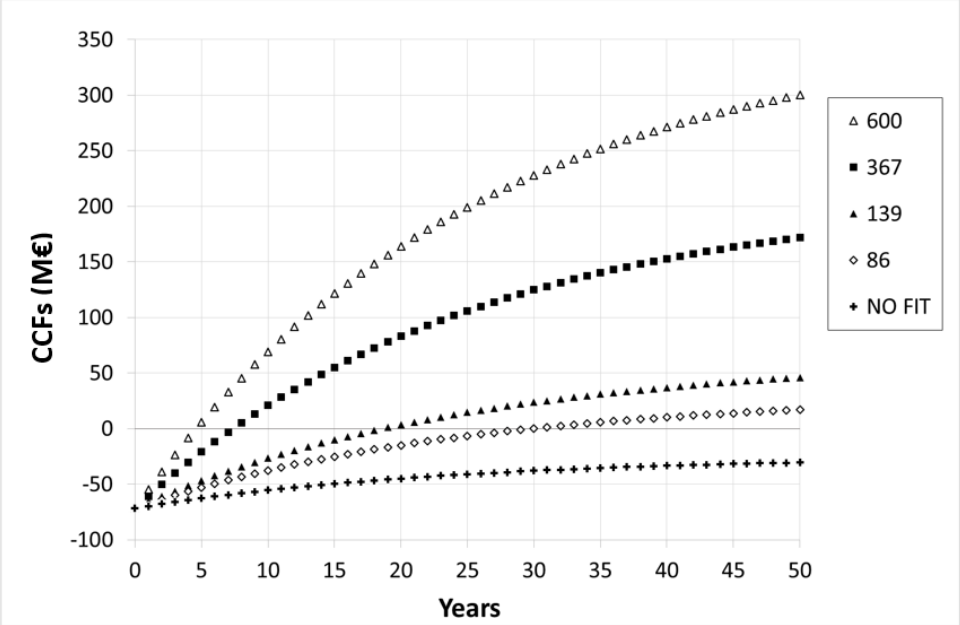

Figure 17. Actualized CCFs (i.e., NPV) of the hybrid plant for different incentive systems on produced wave energy.

Table 14. Results from the economic assessment of the hybrid plant with different support schemes for wave energy production.

FIT on wave energy (€/MWh)	0	86	139	367	600
PBP (y)	37	17	13	6	4
NPV (M€)	-44.85	-14.87	3.60	83.07	164.28

7. Conclusions

This paper started from addressing jointly three key observations: the integration of RES, and particularly of non-contemporaneous RES, may allow to maximise RES production while minimising environmental and economic impacts; most islands are still dependent on expensive fuel imports and are exposed to water scarcity and increasing touristic pressures, requiring the development of desalinisation plants that are energetically demanding; the local use of RES instead of the connection to the grid may allow to overcome technological and economic barriers for off-shore installations.

With this aim, the paper analysed the integration of different renewable resources, specifically wave and solar energy, to power a desalinisation plant in the touristic island of Tenerife.

719 The paper presented an original procedure for the study of RES integration, based on three
720 consecutive steps. The first one consists in the assessment of the available RES, the second is the
721 evaluation of the optimal RES mixing and the third one consists in a preliminary economic evaluation
722 of the hybrid system. This methodology is not site specific and is not dependent neither on the type
723 of RES and on the devices employed, nor on the characteristics of the external power load.

724 In the first step, the yearly available energy and potential production from waves and sun was
725 estimated based on literature data. The yearly average wave power in the North-East of Tenerife is
726 18.54 kW/m, with no significant variation over the examined period 1958-2018. A yearly energy
727 production of 13.2 GWh/y is obtained by installing a WD device at a depth of about 50 m and at a
728 distance from shore of about 4 km, in a favourable location for WECs deployment. Contrary to
729 expectations, the energy production of the WD is almost equally distributed over the different
730 seasons. The annual average hourly solar irradiance in in the area of Santa Cruz is over 400 W/m^2,
731 with peaks in Spring and Summer, and it is stable across the decades both from an annual and a
732 seasonal point of view. The annual electricity production from a medium-efficiency PV panel is of
733 320.6 $kWh/m^2/y$.

734 In the second step, the optimal RES mixing is determined as the combination of devices that
735 maximises the time during which the energy needs are satisfied by RES only. The assessment is
736 carried out based on the hourly RES availability, on the devices hourly producibility and on the
737 hourly energy requirements of the external activity.

738 In particular, the mixing of wave and solar energy to supply a desalination plant was here designed,
739 to cover the plant energy requirements by means of RES only for the majority of the time, while
740 contemporarily minimizing the RES peaks and storage needs. To fill the energy valleys, a proper
741 back-up system is designed, consisting of a low-duty simple-cycle gas turbine. The combination of
742 energy generation by two WDs and an area of 35’000 m^2 of PV-panels area reduces to 15% the time
743 period over which the RESs are insufficient to provide the power supply to the 2MW desalinisation
744 plant in Tenerife.

745 This optimal mixing criterion can be applied to any RES combination and in any site. Depending on
746 the application, the variability of energy requirements at different timescales has to be considered.
747 For a more detailed evaluation, energy losses should also be taken into account.

In the third step, a generic framework for a preliminary economic evaluation of the hybrid system is provided, by identifying the most important economic indicators and by describing a procedure for the assessment of economic balance. The framework takes into account some key parameters, such as government incentives, and can support the scenario analysis for a promising development of such hybrid plants at any location.

Specifically, the preliminary economic assessment of the examined integrated RES installation in Tenerife shows that the LCOE of each resource after 20 years (53.31 €/MWh for solar energy and 261 €/MWh for wave energy) falls within the respective typical ranges which can be found in recent literature. The pay-back period of the investment for the hybrid plant is of 39 years and may decrease to less than 20 years in case of government incentives, such as the FIT, that could significantly increase the confidence towards innovative energy transition projects.

Acknowledgments

This research is part of the PON Project “Off-shore Platform Conversion for Eco-sustainable Multiple Uses” (PlaCE) 2018-2021 (https://bluegrowth-place.eu/), supported by the Italian Ministry of Education, University and Research and funded by the European Union.

References

Access to land (2013) Background: land. Available at: https://www.accesstoland.eu/Background-Land-23 (Accessed: 24 August 2020).

Agora Energiewende (2015) Current and Future Cost of Photovoltaics. Available at: https://www.ise.fraunhofer.de/content/dam/ise/de/documents/publications/studies/AgoraEnergiewende_Current_and_Future_Cost_of_PV_Feb2015_web.pdf (Accessed: 24 August 2020).

Astariz, S., Perez-Collazo, C., Abanades, J. & Iglesias, G., 2015. Co-located wind-wave farm synergies (Operation & Maintenance): A case study. Energy Conversion and Management 91 (2015) 63–75.

Berenguel-Felices F., Lara-Galera A. and Muñoz-Medina M. B., 2020. Requirements for the Construction of New Desalination Plants into a Framework of Sustainability. *Sustainability*, **2020**, 12, 5124; doi:10.3390/su12125124.

Cabildo de Tenerife (2019) Red Canaria de Espacios Naturales Protegidos de la Isla de Tenerife. Available at: https://www.tenerife.es/portalcabtfe/es/temas/medio-ambiente-de-tenerife/espacios-naturales-protegidos/red-canaria-de-espacios-naturales-protegidos-de-la-isla-de-tenerife (Accessed: 21 April 2020).

Canadian Solar (2020) Datasheet PV module- CS6K-260-265-270-275.

Carbon Trust, 2005. Variability of UK Marine Resources: an assessment of the variability characteristics of the UK's wave and tidal current power resources and their implications for large scale development scenarios. Commissioned by The Carbon Trust and Produced by the Environmental Change Institute, July 2005

Carniel, R. et al. (2008) 'The seismic noise at Las Cañadas volcanic caldera, Tenerife, Spain: Persistence characterization, and possible relationship with regional tectonic events', Journal of Volcanology and Geothermal Research, 173 (1–2), pp. 157–164. doi: 10.1016/j.jvolgeores.2007.12.044.

Carrillo M., Pérez-Vallazza C., Alvarez-Vazquez R., Cetacean diversity and distribution off Tenerife (Canary Islands). Marine Biodiversity Records, © Marine Biological Association of the United Kingdom, Vol. 3; e97; 2010. doi:10.1017/S1755267210000801.

Carta J. A., González J., Cabrera P., Subiela V. J., 2015. Preliminary experimental analysis of a small-scale prototype SWRO desalination plant, designed for continuous adjustment of its energy consumption to the widely varying power generated by a stand-alone wind turbine. Applied Energy 137 (2015) 222–239.

CEICC, 2016. Anuario Energético de Canarias 2014, s.l.: Consejería de Economía, Industria, Comercio y Conocimiento − Gobierno de Canarias

Cipollina A., Tzen E., Subiela V., Papapetrou M., Koschikowski J., Schwantes R., M. Wieghaus M., Zaragoza G., 2014. Renewable energy desalination: performance analysis and operating data of existing RES desalination plants. Desalination and Water Treatment (2014) 1–21. doi: 10.1080/19443994.2014.959734

CityPopulation (2020) Santa Cruz de Tenerife. Available at: https://www.citypopulation.de/en/spain/canarias/santa_cruz_de_tenerife/38038__santa_cruz_de_tenerife/ (Accessed: 12 October 2020).

Clean energy for EU islands, 2017. Political Declaration on Clean Energy for EU Islands, https://euislands.eu/ (accessed December 2020)

Clean energy for EU islands, 2020. Memorandum of Understanding on the Clean energy for EU islands initiative, https://ec.europa.eu/info/sites/info/files/energy_climate_change_environment/news/documents/mou_of_split_june_2020.pdf (accessed December 2020)

Contestabile, P., Lauro, E. D., Galli, P., Corselli, C., & Vicinanza, D. (2017). Offshore wind and wave energy assessment around Malè and Magoodhoo Island (Maldives). Sustainability, 9(4), 613.

Culson, J. M. and Richardson, J. F. (2017) Culson and Richardson's Chemical Engineering. 7th edn. Edited by R. P. Chhabra and V. Shankar. Butterworth-Heinemann.

Dorta, P. 2007. Catálogo de riesgos climáticos en Canarias: amenazas y vulnerabilidad, Geographicalia, 51, 133-160.

Drew, B., Plummer, A. R. and M. Sahinkaya, 2009. A review of wave energy converter technology, Proceedings of the Institution of Mechanical Engineers Part A Journal of Power and Energy 223(8):887-902

Durning, B. and Broderick, M. 2019. Development of cumulative impact assessment guidelines for offshore wind farms and evaluation of use in project making, Impact Assessment and Project Appraisal, 37 (2), 124-138.

ECMWF (2020) Copernicus Climate Data Store. Available at: https://cds.climate.copernicus.eu/cdsapp#!/home (Accessed: 17 April 2020).

EMCWF (2020) ERA5 hourly data on single levels from 1979 to present. Available at: https://cds.climate.copernicus.eu/cdsapp#!/dataset/reanalysis-era5-single-levels?tab=overview (Accessed: 21 April 2020).

Eskilsson C., Palm J., Kofoed J.P., Friis-Madsen E., 2014. CFD study of the overtopping discharge of the Wave Dragon wave energy converter. 1st RENEW Conference, Lisbon, 2014.

EuropaPress (2019) La ampliación de la desaladora de Santa Cruz de Tenerife permitirá tratar casi 29.000 metros cúbicos diarios de agua. Available at: https://www.europapress.es/islas-canarias/noticia-ampliacion-desaladora-santa-cruz-tenerife-permitira-tratar-casi-29000-metros-cubicos-diarios-agua-20190225170523.html (Accessed: 2 September 2020).

Faiman, D. (2008) 'Assessing the Outdoor Operating Temperature of Photovoltaic Modules David', PROGRESS IN PHOTOVOLTAICS: RESEARCH AND APPLICATIONS, 16, pp. 307–315. doi: 10.1002/pip.

Fathima, A. H. and Palanisamy, K. (2018) Renewable systems and energy storages for hybrid systems, Hybrid-renewable energy systems in microgrids: Integration, developments and control. Elsevier Ltd. doi: 10.1016/B978-0-08-102493-5.00008-X.

838 Fernandez Chozas, J., Helstrup Jensen, N.E. & Sørensen, H.C. Economic benefit of combining wave and wind
839 power productions in day-ahead electricity markets. In Proceedings of the 4th International
840 Conference on Ocean Energy, ICOE, Dublin, Ireland, 17-19 October 2012.

841 Fernandez-Chozas J., Kofoed J. P. & Jensen N. E. H., 2014. DCE Technical Report N. 161, User guide – The COE
842 Calculation Tool for Wave Energy Converters (Version 1.6, April 2014), Aalborg University,
843 Department of Civil Engineering, Wave Energy Research Group.

844 Fernandez Prieto L., Rodriguez Rodriguez G., Shallenberg Rodriguez J., 2019. Wave energy to power a
845 desalination plant in the north of Gran Canaria Island: Wave resource, socioeconomic and
846 environmental assessment. Journal of Environmental Management 231 (2019) 546–551.
847 https://doi.org/10.1016/j.jenvman.2018.10.071

848 Four Peaks Technologies (2019) Solar Electricity Costs. Available at:
849 http://solarcellcentral.com/cost_page.html (Accessed: 24 August 2020).

850 Franzitta V., Curto D., Milone D. and Viola A., 2016. The Desalination Process Driven by Wave Energy: A
851 Challenge for the Future. Energies 2016, 9, 1032; doi:10.3390/en9121032.

852 Frigaard, P. B., Andersen, T. L., Kofoed, J. P., Kramer, M. M., & Ambühl, S. (2016). *Wavestar Energy Production*
853 *Outlook*. Department of Civil Engineering, Aalborg University. DCE Technical reports, No. 201

854 Friis-Madsen E., Soerensen H. C. & Russel I., 2018. "Small is beautiful" – but will small WECs ever become
855 commercial? , ICOE 12-14 June 2018, Cherbourg, France.

856 Fu, R., Feldman, D. and Margolis, R. (2018) U.S. Solar Photovoltaic System Cost Benchmark: Q1 2018,
857 Technical Report: NREL/TP-6A20-72399. Available at:
858 https://www.nrel.gov/docs/fy19osti/72399.pdf.

859 Miguel A. García-Rubio & Jorge Guardiola (2012) Desalination in Spain: A Growing Alternative for Water
860 Supply, International Journal of Water Resources Development, 28:1, 171-186, DOI:
861 10.1080/07900627.2012.642245

862 GlobalPetrolPrices (2020a) Natural Gas prices. Available at:
863 https://www.globalpetrolprices.com/natural_gas_prices/ (Accessed: 20 September 2020).

864 GlobalPetrolPrices (2020b) Spain electricity prices. Available at:
865 https://www.globalpetrolprices.com/Spain/electricity_prices/ (Accessed: 9 September 2020).

866 Gobierno de Canarias (2017) Anuario Energético de Canarias 2016.

867 Gobierno de Canarias (2017) Estrategia Energetica de Canarias 2015-2025. Available at:
868 https://www.gobiernodecanarias.org/energia/temas/planificacion/.

869 Gobierno de Canarias (2020a) Sistema de information territorial de Canarias. Available at:
870 https://visor.grafcan.es/visorweb/ (Accessed: 22 October 2020).

871 Gobierno de Canarias (2020b) Turismo de Islas Canarias. Available at: https://turismodeislascanarias.com/es/
872 (Accessed: 4 July 2020).

873 Goncalves M., Martinho P. & Soares G. C., 2014. Assessment of wave energy in the Canary Islands. Renewable
874 Energy 68 (2014) 774-784.

875 Goncalves M., Martinho P. & Soares G. C., 2020. Wave energy assessment based on a 33-year hindcast for
876 the Canary Islands. Renewable Energy, **152**, 259-269.

877 Gonzalez-Salazar, M. A., Kirsten, T. and Prchlik, L. (2018) 'Review of the operational flexibility and emissions
878 of gas- and coal-fired power plants in a future with growing renewables', Renewable and Sustainable
879 Energy Reviews. Elsevier Ltd, 82(July 2017), pp. 1497–1513. doi: 10.1016/j.rser.2017.05.278.

880 Guaita-Pradas, I. and Blasco-Ruiz, A. (2020) 'Analyzing profitability and discount rates for solar PV Plants. A
881 spanish case', Sustainability (Switzerland), 12(8). doi: 10.3390/SU12083157.

882 Hannon, M. Topham, E. MacMillan,D. Dixon, J. Collu, M. 2019. Offshore wind, ready to float? Global and UK
883 trends in the floating offshore wind market. University of Strathclyde, Glasgow,
884 https://doi.org/10.17868/69501

885 Harris R.E., Johanning L., Wolfram J., 2006. Mooring systems for wave energy converters: A review of design
886 issues and choices, Proc. of the Institution of Mechanical Engineers Part B Journal of Engineering
887 Manufacture 220(4):159-168

888 Henderson, R. Design, simulation, and testing of a novel hydraulic power take-off system for the Pelamis
889 wave energy converter. Renew. Energy 2006, 31, 271–283.

890 Hernandez J. C., Clemente S., Sangil C. and Brito A., 2007. Actual status of the sea urchin Diadema aff.
891 antillarum populations and macroalgal cover in marine protected areas compared to a highly fished
892 area (Canary Islands – eastern Atlantic Ocean). Aquatic Conser*v*: Mar. Freshw. Ecosyst. (2007)
893 Published online in Wiley InterScience (www.interscience.wiley.com) DOI: 10.1002/aqc.903.

894 Hernandez, Y., Guimarães Pereira, A. and P. Barbosa, 2018. Resilient futures of a small island: A participatory
895 approach in Tenerife (Canary Islands) to address climate change. Environmental Science & Policy, 80,
896 28-37.

897 Huld, T. et al. (2011) 'A power-rating model for crystalline silicon PV modules', Solar Energy Materials and
898 Solar Cells. Elsevier, 95(12), pp. 3359–3369. doi: 10.1016/j.solmat.2011.07.026.

899 Ipieca (2014) Open Cycle Gas Turbines. Available at: https://www.ipieca.org/resources/energy-efficiency-
900 solutions/power-and-heat-generation/open-cycle-gas-turbines/ (Accessed: 20 September 2020).

901 ITER, I. T. y de E. renovables (2016) Photovoltaic installations. Available at: https://www.iter.es/portfolio-
902 items/plantas-fotovoltaicas/?lang=en (Accessed: 17 April 2020).

903 Jäger-Waldau, A. (2019) PV Status Report 2019, EUR 29938, Publications Office of the European Union. doi:
904 10.2760/326629.

905 Jimeno M. (2019), Tenders (Régimen retributivo especifico), RES LEGAL Europe: Legal Sources on Renewable
906 Energy, http://www.res-legal.eu/search-by-country/spain/single/s/res-e/t/promotion/aid/feed-in-
907 tariff-regimen-especial/lastp/195/ (accessed 04 December 2020).

908 Kausche, M., Adam, F., Dahlhaus, F. and Grossmann, J. 2018. Floating offshore wind - Economic and ecological
909 challenges of a TLP solution, Renewable Energy 126, DOI: 10.1016/j.renene.2018.03.058

910

Khare, A. (2020) 'A critical review on the efficiency improvement of upconversion assisted solar cells', Journal of Alloys and Compounds. Elsevier B.V, 821, p. 153214. doi: 10.1016/j.jallcom.2019.153214.

Koehl, M. et al. (2011) 'Modeling of the nominal operating cell temperature based on outdoor weathering', Solar Energy Materials and Solar Cells. Elsevier, 95(7), pp. 1638–1646. doi: 10.1016/j.solmat.2011.01.020.

Kofoed, J.P.; Frigaard, P.; Friis-Madsen, E.; Sørensen, H.C. Prototype testing of the wave energy converter Wave Dragon. Renew. Energy 2006, 31, 181–189.

Kost, C. et al. (2018) Levelized Cost of Electricity - Renewable Energy Technologies, Fraunhofer ISE.

Lauer, M. (2008) Methodology guideline on techno economic assessment (TEA), Intelligent Energy Europe. Available at: https://ec.europa.eu/energy/intelligent/projects/sites/iee-projects/files/projects/documents/thermalnet_methodology_guideline_on_techno_economic_assessment.pdf.

Leijon J. And Boström C., 2018. Freshwater production from the motion of ocean waves – A review. Desalination 435 (2018) 161–171.

Llanes P., Muñoz A., Muñoz-Martin A., Acosta J., Herranz P., Carbo A., Palomo C. & ZEE Working Group, 2003. Morphological and structural analysis in the Anaga offshore massif, Canary Islands: fractures and debris avalanches relationships. Marine Geophysical Researches (2003) 24: 91–112 DOI 10.1007/s11001-004-1335-3.

Lüdeke, J. 2017. Offshore Wind Energy: Good Practice in Impact Assessment, Mitigation and Compensation, Journal of Environmental Assessment Policy and Management 19(1):31

Margolis, R., Feldman, D. and Boff, D. (2020) 'Solar Industry Update', National Renewable Energy Laboratory, (May 28), pp. 1–83. doi: NREL/PR-6A20-68425.

MARINA: Marine Renewable Integrated Application Platform (Jan 2010 – Jun 2014) https://cordis.europa.eu/project/id/241402 (accessed 04 December 2020)

Marine Conservation Institute, Marine Protection Atlas. https://mpatlas.org/zones/68812757/map (accessed 02 October 2020).

Martinelli, L. and Zanuttigh, B. 2018. Effects of Mooring Compliancy on the Mooring Forces, Power Production, and Dynamics of a Floating Wave Activated Body Energy Converter, Energies 2018, 11(12), 3535

Moor A., Price J. & Zeyringer M., 2018. The Role of Floating Offshore Wind in a Renewable Focused Electricity System for Great Britain in 2050, Energy Strategy Reviews 22: 270-278, November 2018.

MUSES: Multi-Use in European Seas (Nov 2016 – Oct 2018) https://cordis.europa.eu/project/id/727451 (accessed 04 December 2020)

Nassar W. M., Anay-Lara O., Ahmed K. H., Campos-Gaona D. and Elgenedy M., 2020. Assessment of Multi-Use Offshore Platforms: Structure Classification and Design Challenges. *Sustainability* **2020**, *12*, 1860; doi:10.3390/su12051860.

947 ORECCA: Off-shore Renewable Energy Conversion platforms – Coordination Action (Mar 2010 – Aug 2011)
948 https://cordis.europa.eu/project/id/241421 (accessed 04 December 2020)

949 Papapetrou M., Cipollina A., La Commare U., Micale G., Zaragoza G., Kosmadakis G., 2017. Assessment of
950 methodologies and data used to calculate desalination costs. *Desalination*, 419 (**2017**) 8–19, DOI:
951 10.1016/j.desal.2017.05.038.

952 Parker, W. S. (2016) 'Reanalyses and observations: What's the Difference?', Bulletin of the American
953 Meteorological Society, 97(9), pp. 1565–1572. doi: 10.1175/BAMS-D-14-00226.1.

954 Pérez Lapeña, B., Wijnberg, K., Hulscher, S. and A. Stein, 2010. Environmental impact assessment of offshore
955 wind farms: a simulation-based approach, J. of Applied Ecology, 47, 1110-1118.

956 Perez-Collazo, C., Greaves, D., Iglesias, G. 2015. A review of combined wave and offshore wind energy,
957 Renew. Sustain. Energy Rev. 42, 141–153.

958 Photovoltaic-software (2019) How to calculate the annual solar energy output of a photovoltaic system?
959 Available at: https://photovoltaic-software.com/principle-ressources/how-calculate-solar-energy-
960 power-pv-systems.

961 PlaCe: Off-shore Platform Conversion for Eco-sustainable Multiple Uses (2018-2021), https://bluegrowth-
962 place.eu/ (Accessed December 2020)

963 Puertos del Estado, Gobierno de Espana, http://www.puertos.es/en-us/oceanografia/Pages/portus.aspx
964 (Accessed November 2020).

965 Real Decreto 1458/2018, de 14 de diciembre, por el que se declaran oficiales las cifras de población
966 resultantes de la revisión del Padrón municipal referidas al 1 de enero de 2019" [Royal Decree
967 1458/2018, of 14 December, by which the population numbers resulting from the review of the
968 municipal register as of 01 January 2019 are declared official] (PDF) (in Spanish). Ministerio de
969 Economía y Empresa. 2019. Retrieved 18 July 2019.

970 Red Electrica de Espana (2014) Press office -Red Eléctrica begins the environmental studies for the submarine
971 electricity interconnection between Tenerife and La Gomera. Available at:
972 https://www.ree.es/en/press-office/press-release/2014/11/red-electrica-begins-environmental-
973 studies-submarine-electricity-interconnection-tenerife-la-gomera (Accessed: 25 June 2020).

974 Red Electrica de Espana (2020) Singularidades del sistema canario. Available at:
975 https://www.ree.es/es/actividades/sistema-electrico-canario/singularidades-del-sistema
976 (Accessed: 25 June 2020).

977 Reuters Events-Renewables (2019) US solar maintenance costs plummet as tech gains multiply. Available at:
978 https://analysis.newenergyupdate.com/pv-insider/us-solar-maintenance-costs-plummet-tech-
979 gains-multiply (Accessed: 24 August 2020).

980 Rosales-Asensio E., Borge-Diez D., Perez-Hoyos A., Colmenar-Santos A., 2019. Reduction of water cost for an
981 existing wind-energy-based desalination scheme: A preliminary configuration. Energy 167 (2019)
982 548-560.

983 Rosales-Asensio, E. et al. (2020) 'Stress mitigation of conventional water resources in water-scarce areas
984 through the use of renewable energy powered desalination plants: An application to the Canary
985 Islands', Energy Reports. Elsevier Ltd, 6 (2020), pp. 124–135. doi: 10.1016/j.egyr.2019.10.031.

986 Sagaseta de Ilurdoz Cortadellas A. M., Rodriguez B., Pereda C., Moreno D., 2011. Preliminary study for the
987 implementation of the "Wave Dragon" in Gran Canaria, Canary Islands, Spain. RE&PQJ, Vol.1, No.9,
988 May 2011. https://doi.org/10.24084/repqj09.560.

989 Sahu, A., Yadav, N. and Sudhakar, K. (2016) 'Floating photovoltaic power plant: A review', Renewable and
990 Sustainable Energy Reviews, 66, pp. 815–824. doi: 10.1016/j.rser.2016.08.051.

991 Schallenberg-Rodríguez, J. and Notario-del Pino, J. (2014) 'Evaluation of on-shore wind techno-economical
992 potential in regions and islands', Applied Energy, 124, pp. 117–129. doi:
993 10.1016/j.apenergy.2014.02.050.

994 Schallenberg-Rodríguez, J., Veza, J. M. and Blanco-Marigorta, A. (2014) 'Energy efficiency and desalination in
995 the Canary Islands', Renewable and Sustainable Energy Reviews, 40, pp. 741–748. doi:
996 10.1016/j.rser.2014.07.213.

997 Schallenberg-Rodríguez, J. and García Montesdeoca, N. (2018) 'Spatial planning to estimate the offshore wind
998 energy potential in coastal regions and islands. Practical case: The Canary Islands', Energy. Elsevier
999 Ltd, 143, pp. 91–103. doi: 10.1016/j.energy.2017.10.084.

1000 Segurado, R., Costa, M. and Duić, N. (2018) Integrated Planning of Energy and Water Supply in Islands,
1001 Renewable Energy Powered Desalination Handbook: Application and Thermodynamics. doi:
1002 10.1016/B978-0-12-815244-7.00009-X.

1003 SHARP (2008) Datasheet SolarNAE_L5_E0514.

1004 Silva D., Bento R. A., Martinho P. & Soares G. C., 2015. High resolution local wave energy modelling in the
1005 Iberian Peninsula. Energy, 91, 1099-1112.

1006 SOFIA: Smart Objects For Intelligent Applications (Jan 2009 – Mar 2012)
1007 https://cordis.europa.eu/project/id/100017 (accessed 04 December 2020)

1008 Sorensen H. C. & Friis-Madsen E., 2015. Wave Dragon 1.5 MW North Sea Demonstrator Phase 1, EUDP J.nr.
1009 64010-0405, September 2015.

1010 SUNPOWER (2020) Datasheet MAXEON 3 - 400 W.

1011 Trapani, K. and Redón-Santafé (2015) 'A review of floating photovoltaic installations : 2007 -2013', Progress
1012 in Photovoltaics, 23, pp. 524–532. doi: 10.1002/pip.2466.

1013 TROPOS: Modular Multi-use Deep Water Offshore Platform Harnessing and Servicing Mediterranean,
1014 Subtropical and Tropical Marine and Maritime Resources (Feb 2012 – Jan 2015)
1015 https://cordis.europa.eu/project/id/288192 (accessed 04 December 2020)

1016 U.S. Energy Information Administration (2018) Construction cost data for electric generators installed in
1017 2018. Available at: https://www.globalpetrolprices.com/natural_gas_prices/ (Accessed: 20
1018 September 2020).

1019 Uche-Soria, M. and C. Rodríguez-Monroy, 2018. Special Regulation of Isolated Power Systems: The Canary
1020 Islands, Spain, Sustainability, 10, 2572; doi:10.3390/su10072572

1021 UNI Standards UNI 8477-1 (1983) Energia solare. Calcolo degli apporti per applicazioni in edilizia. Valutazione
1022 dell'energia raggiante ricevuta.

1023 UNI Standards UNI/TS 11300-4 (2016) Prestazioni energetiche degli edifici - Parte 4: Utilizzo di energie
1024 rinnovabili e di altri metodi di generazione per la climatizzazione invernale e per la produzione di
1025 acqua calda sanitaria.

1026 Veigas M. and Iglesias G., 2013. Wave and offshore wind potential for the island of Tenerife. Energy
1027 Conversion and Management 76 (2013) 738-745.

1028 Verdolini, E., Vona, F. and Popp, D. (2018) 'Bridging the gap: Do fast-reacting fossil technologies facilitate
1029 renewable energy diffusion?', Energy Policy, 116(February), pp. 242–256. doi:
1030 10.1016/j.enpol.2018.01.058.

1031 Vidalic, H. (2019) France: Tarif d´achat, RES LEGAL. Available at: http://www.res-legal.eu/search-by-
1032 country/france/single/s/res-e/t/promotion/aid/feed-in-tariff-tarif-dachat/lastp/131/ (Accessed: 10
1033 November 2020).

1034 Volcano Discovery (2020) Earthquakes in Canary Islands. Available at:
1035 https://www.volcanodiscovery.com/earthquakes/canaries.html (Accessed: 22 June 2020).

1036 WADE (2020) Gas Turbines. Available at: http://www.localpower.org/deb_tech_gt.html (Accessed: 20
1037 September 2020).

1038 Wind Power Hub project, https://northseawindpowerhub.eu/ (accessed 02 December 2020)

1039 World seaports catalogue, marine and seaports market place. http://ports.com/sea-route/ (accessed 04
1040 December 2020).

1041 Yemm R., Pizer D., Retzler C., Henderson R., 2012. Pelamis: experience from concept to connection. Phil.
1042 Trans. R. Soc. A (2012) 370, 365–380. doi:10.1098/rsta.2011.0312

1043 Zanuttigh B., Martinelli L., Castagnetti M., Ruol P., Kofoed J. P., Frigaard P., 2010. Integration of wave energy
1044 converters into coastal protection schemes. 3rd International Conference on Ocean Energy, 6
1045 October 2010 Bilbao.

1046 Zanuttigh, B.; Angelelli, E.; Bellotti, G.; Romano, A.; Krontira, Y.; Troianos, D.; Suffredini, R.; Franceschi, G.;
1047 Cantù, M.; Airoldi, L.; Zagonari, F.; Taramelli, A.; Filipponi, F.; Jimenez, C.; Evriviadou, M.; Broszeit, S.
1048 2015. Boosting Blue Growth in a Mild Sea: Analysis of the Synergies Produced by a Multi-Purpose
1049 Offshore Installation in the Northern Adriatic, Italy. Sustainability, 7, 6804-6853.

1050 Zanuttigh B., Angelelli E., Kortenhaus A., Koca K., Krontira Y. and P. Koundouri, 2016. METHODOLOGY FOR
1051 MULTI-CRITERIA DESIGN OF MULTI-USE OFF-SHORE PLATFORMS FOR MARINE RENWABLE ENERGY
1052 HARVESTING, Renewable Energy, 85, 1271-1289.

1053 Zanuttigh, B., Palma, G., Brizzi, G., Bellotti, G., Romano, A. & Suffredini R., 2021. Design of a multi-use marine
1054 area off-shore the Mediterranean Sea, Ocean Eng., 221, 108515

1055